NAVAL POSTGRADUATE SCHOOL

Monterey, California

THESIS

AN EXPERIMENTAL STUDY OF COLLECTIVE SEA STATE MODES OF DEEP WATER SURFACE GRAVITY WAVES

by

Patricia A. Gill

December 1994

Thesis Advisor: Robert M. Keolian
Thesis Co-Advisor: Andrés Larraza

Approved for public release; distribution is unlimited

REPORT DOCUMENTATION PAGE

Form Approved
OMB No. 0704-0188

1. AGENCY USE ONLY *(Leave blank)*	2. REPORT DATE	3. REPORT TYPE AND DATES COVERED
	December 1994	Master's Thesis

4. TITLE AND SUBTITLE
AN EXPERIMENTAL STUDY OF COLLECTIVE SEA STATE MODES OF DEEP WATER SURFACE GRAVITY WAVES

5. FUNDING NUMBERS
PE 0601153N
G N0001494WR23019
TA 312s003-03

6. AUTHOR(S)
Patricia A. Gill

7. PERFORMING ORGANIZATION NAME(S) AND ADDRESS(ES)
Naval Postgraduate School
Monterey CA 93943-5000

8. PERFORMING ORGANIZATION REPORT NUMBER

9. SPONSORING/MONITORING AGENCY NAME(S) AND ADDRESS(ES)
Office of Naval Research
Code 331
800 N. Quincy Street
Arlington, VA 22217-5660

10. SPONSORING/MONITORING AGENCY REPORT NUMBER

11. SUPPLEMENTARY NOTES
The views expressed in this thesis are those of the author and do not reflect the official policy or position of the Department of Defense or the U.S. Government.

12a. DISTRIBUTION/AVAILABILITY STATEMENT
Approved for public release; distribution is unlimited.

12b. DISTRIBUTION CODE

13. ABSTRACT ***(maximum 200 words)***

Experimental tests of the theory of collective sea state modes of deep water surface gravity waves were made in a 20 meter long, 1.1 meter wide wind-wave tank. First, bursts of broadband wave energy were injected into the upwind end of the tank with a paddle. According to wave turbulence theory and previous experiments, it is expected that the collective mode can be seen as a change in the wind generated background spectral density propagating down the tank. The collective mode is expected to give an anomalous phase shift between the wind generated waves and the lowest tank modes. A series of experiments were conducted to measure the phase of the lowest oscillatory modes of the tank at which increases in the magnitude of wind generated waves occurred. Finally, the surface tension of water in the tank was measured in order to better characterize our system. Although our experiments suggest that the collective mode may indeed exist, the results, so far, remain inconclusive.

14. SUBJECT TERMS
Collective Mode, Surface Gravity Waves, Wind-Wave Tank, Surface Tension, Fundamental Mode

15. NUMBER OF PAGES
65

16. PRICE CODE

17. SECURITY CLASSIFICATION OF REPORT	18. SECURITY CLASSIFICATION OF THIS PAGE	19. SECURITY CLASSIFICATION OF ABSTRACT	20. LIMITATION OF ABSTRACT
Unclassified	Unclassified	Unclassified	UL

NSN 7540-01-280-5500

Standard Form 298 (Rev. 2-89)
Prescribed by ANSI Std. 239-18
298-102

Approved for public release; distribution is unlimited.

AN EXPERIMENTAL STUDY OF COLLECTIVE SEA STATE MODES OF DEEP WATER SURFACE GRAVITY WAVES

by

Patricia A. Gill
Lieutenant, United States Navy
B.S., United States Naval Academy, 1988

Submitted in partial fulfillment of the
requirements for the degree of

MASTER OF SCIENCE IN APPLIED PHYSICS

from the

NAVAL POSTGRADUATE SCHOOL
December 1994

Author: Patricia A. Gill
Patricia A. Gill

Approved by: Robert Keolian
Robert M. Keolian, Thesis Advisor

Andrés Larraza, Thesis Co-Advisor

W. B. Colson
William B. Colson, Chairman
Department of Physics

Accesion For	
NTIS CRA&I	X
DTIC TAB	☐
Unannounced	☐
Justification	
By	
Distribution /	
Availability Codes	
Dist	Avail and / or Special
A-1	

ABSTRACT

Experimental tests of the theory of collective sea state modes of deep water surface gravity waves were made in a 20 meter long, 1.1 meter wide wind-wave tank. First, bursts of broadband wave energy were injected into the upwind end of the tank with a paddle. According to wave turbulence theory and previous experiments, it is expected that the collective mode can be seen as a change in the wind generated background spectral density propagating down the tank. The collective mode is expected to give an anomalous phase shift between the wind generated waves and the lowest tank modes. A series of experiments were conducted to measure the phase of the lowest oscillatory modes of the tank at which increases in the magnitude of wind generated waves occurred. Finally, the surface tension of water in the tank was measured in order to better characterize our system. Although our experiments suggest that the collective mode may indeed exist, the results, so far, remain inconclusive.

TABLE OF CONTENTS

ACKNOWLEDGMENT

I would like to acknowledge the financial support of the Office of Naval Research. This work was performed under Contract N0001494WR23019.

I would also like to thank my entire family for their support and encouragement over the last year. Thanks to Michael, my husband, for showing me there is more to life than just studying.

Special thanks to LCDR Dave Ekker, USN and LCDR John Davies, CDN Forces for answering all those thesis questions that kept "popping" up. Thanks to my father-in-law, Mike, for proofreading my thesis, to Dave Grooms for constructing the second paddle on the tank, and to George Jaksha for his guidance in using various tools.

Finally, thanks to Professors Keolian and Larraza for their interesting discussions in which I always seemed to learn something new. But, most of all, thanks to Professor Keolian for his patience in explaining many aspects of this thesis and allowing me to work things out at my own speed.

I. INTRODUCTION

This thesis is part of a continuing experimental study of wave turbulence (Zakharov et. al., 1992), a theory of the collective effect of nonlinear interactions among waves. Experiments were conducted in a controlled laboratory wind-wave tank, the Ocean Acoustic Wave Facility at the Naval Postgraduate School, and analyzed using various computer techniques and data-processing programs. It was the goal of this experiment to further clarify the existence and propagation characteristics of a "collective mode" predicted by Larraza (1993) and Larraza and Falkovich (1993) and described in previous experimental studies (Lawrence, 1992 and Davies, 1994). Wave turbulence theory predicts that when a system that supports waves is driven sufficiently off equilibrium by a steady input of energy at short wavelengths, an "inverse cascade" of energy from short to long wavelengths will give rise to a steady state power law spectrum. This theory assumes a state of wave motion characterized by a spectrum where the bandwidth of frequencies is broad, and where the redistribution of energy dominates those processes which bring about thermodynamic equilibrium. Due to the numerous similarities to the theory of hydrodynamic turbulence, this state is called *wave turbulence*.

Larraza and co-workers (Larraza et. al., 1990; Larraza, 1993; Larraza and Falkovich, 1993) have studied the effects of disturbing or spatially modulating the background energy distribution. They have predicted that perturbations of the background spectrum propagate in space as a *collective mode* instead of relaxing back to equilibrium exponentially. The mode is a *wave in the density of waves.* The randomly interacting short waves that form the chop on the ocean surface is considered to be like a "gas" of waves. Nonlinear interactions among the waves cause this gas to act collectively, with its own elasticity and inertia, leading to an independent mode that can propagate. This mode should appear as a *wave of sea state* and may be excited by a passing long wave swell, or by other disturbances.

The wave vector and frequency of the wave are related by the dispersion relation, which for a gravity wave on a fluid of infinite depth is

$$\omega^2 = gk, \tag{1.1}$$

and for the collective mode is

$$\omega = c_{cm}k, \tag{1.2}$$

where ω is the angular frequency, g is the acceleration due to gravity, k is the wave number and c_{cm} is the speed of the collective mode. The dispersion relations for ordinary gravity waves and the collective mode are shown in Figure 1-1. Because of Landau damping (Larraza and Falkovich, 1993), the collective mode is thought to become heavily damped in and beyond the region where the two modes cross, represented by the dashed line in the figure.

By exploiting the difference in the dispersion relations between gravity waves and the collective mode, the collective mode is hoped to be experimentally separated from the deep water surface gravity waves. This separation and observance of the collective mode propagating independently would provide conclusive evidence for the existence of a collective mode.

The experimental study was conducted in a large water tank with fans to create a wind driven background sea state or "chop" and computer controlled mechanical paddles to create a disturbance in the form of either additional chop or of a low frequency "swell." By launching a pulse of noise from a paddle, the propagation characteristics and the phase velocity of the collective mode can in principle be determined by the evolution of the energy spectrum measured at various positions along the tank. It was believed to have been shown in earlier experiments (Lawrence, 1992) that the collective mode could be excited in a controlled laboratory tank by launching modulated noise pulses from a paddle into a broadband background of wind-generated gravity waves. In this case, it was required that the duration time of the modulation be much smaller than the collision time but larger than the period of the individual noise components.

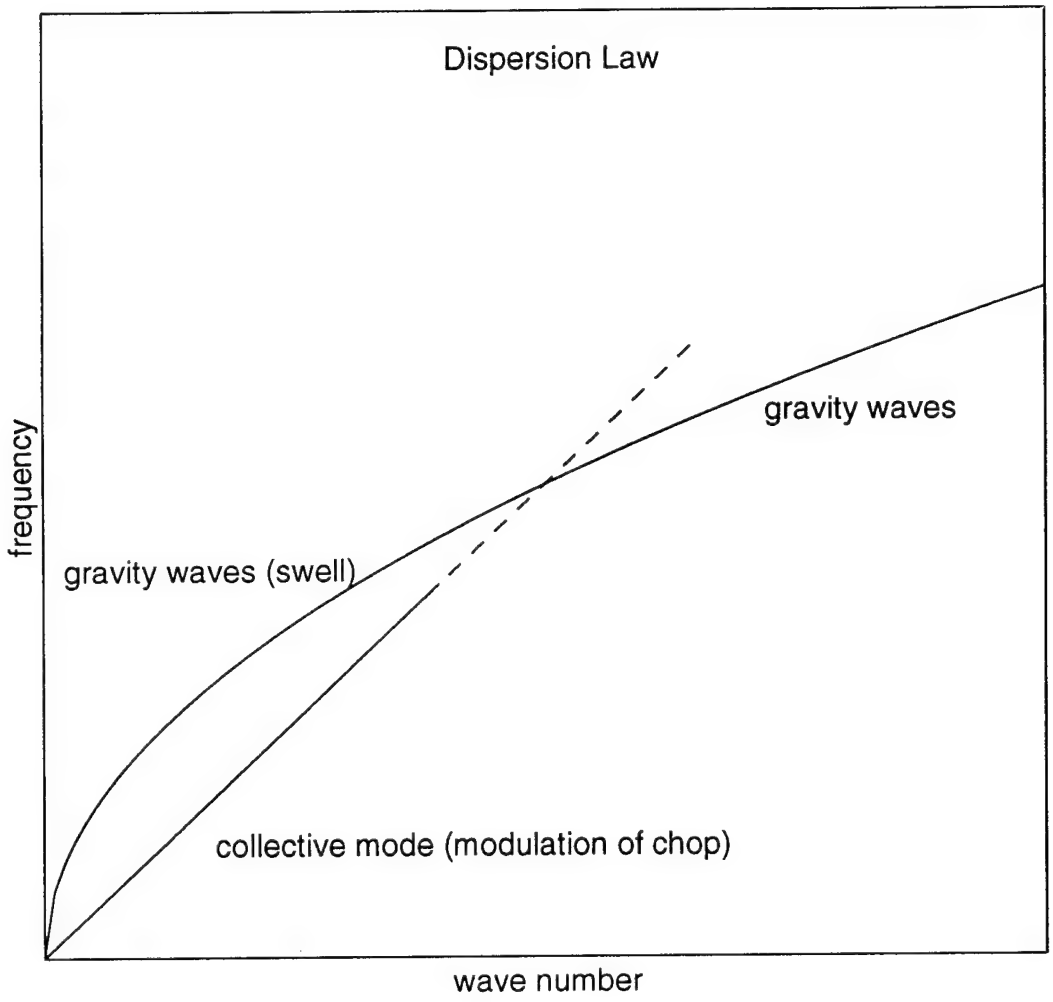

Figure 1-1. Dispersion Law.
A comparison of the Dispersion Law of Gravity Waves and the Collective Mode. The dashed line represents an area of Landau damping.

Because the collective mode is dispersionless, all Fourier components launched in a burst by the paddle that couple to the collective mode should arrive at a position down the tank at the same time. However, because of the dispersion of gravity waves, those Fourier components from the paddle that couple to the gravity wave mode arrive at different times, depending on their frequency. The correct time was calculated using the relationship between frequency and wave number for deep water gravity waves. From the dispersion relationship for deep surface gravity waves expressed earlier as $\omega^2 = gk$, it can be shown that the group velocity, c_g, is one half the phase velocity, c_p. By differentiation:

$$c_g = \frac{d\omega}{dk} \tag{1.3}$$

and since

$$c_p = \frac{\omega}{k} = \frac{g}{\omega}, \tag{1.4}$$

then

$$c_g = \frac{1}{2} c_p = \frac{1}{2}\frac{g}{\omega}. \tag{1.5}$$

A burst of gravity waves propagates at the speed c_g which goes as ω^{-1}. Therefore, the "Time of Flight," as it was referred to by Lawrence (1992), required for the burst to propagate past the wave probe becomes proportional to the natural frequency f:

$$T = \frac{d}{c_g} = \frac{d}{(g/2\omega)} = \frac{2\omega d}{g} = \frac{2 \cdot 2\pi f \cdot d}{g} = \frac{4\pi d}{g} f \quad , \tag{1.6}$$

where d is the distance between probe and paddle.

II. APPARATUS

A. WIND-WAVE TANK SYSTEM

The main apparatus for this experiment is a water tank 20 meters long and 1.1 meters wide. The overall tank layout is shown in Figure 2-1. There are paddles at either end of the tank. A fan box directs wind over the water along a covered wind tunnel section. The nominal distance between the ceiling of the wind tunnel and the water surface is 0.22 meters and the depth of the water in this region is 1.0 meters. The tank opens up into an anechoic section, used in the past to study underwater sound, which is 3.05 meters long, 3.05 meters wide, and 2.90 meters deep sunk into the ground. Additional changes were made to the tank configuration in order to provide a more uniform transition of the waves from the wind tunnel to the anechoic section. First, an airfoil was placed approximately 17 meters from the fan box at the end of the wind tunnel in order to draw the airflow away from the surface making it easier to interpret data results when the probe is in positions three or four of the tank. Also a deeper side wall, 13.5 centimeters above the surface and 34.5 centimeters below the surface, was constructed and placed in the anechoic section so that the tank width was more or less the same for the entire length of the tank. There still exists a discontinuity in the width of the tank at the transition point of wind tunnel to anechoic section, but it is slight.

B. WATER MAINTENANCE

The surface of the water is cleaned by a swimming pool skimming filter installed in the expanded area of the tank. A pump draws a suction on the surface filter, and discharges through a T-valve to a sand filter that removes particulates from the water. The filtered water is carried back to the opposite end of the tank by piping along the side of the tank. The T-valve on the discharge side of the pump can be used to drain the tank by directing the discharge to the building sewage line. The water level is controlled with a toilet float valve to make up for the sizable evaporation caused by the wind.

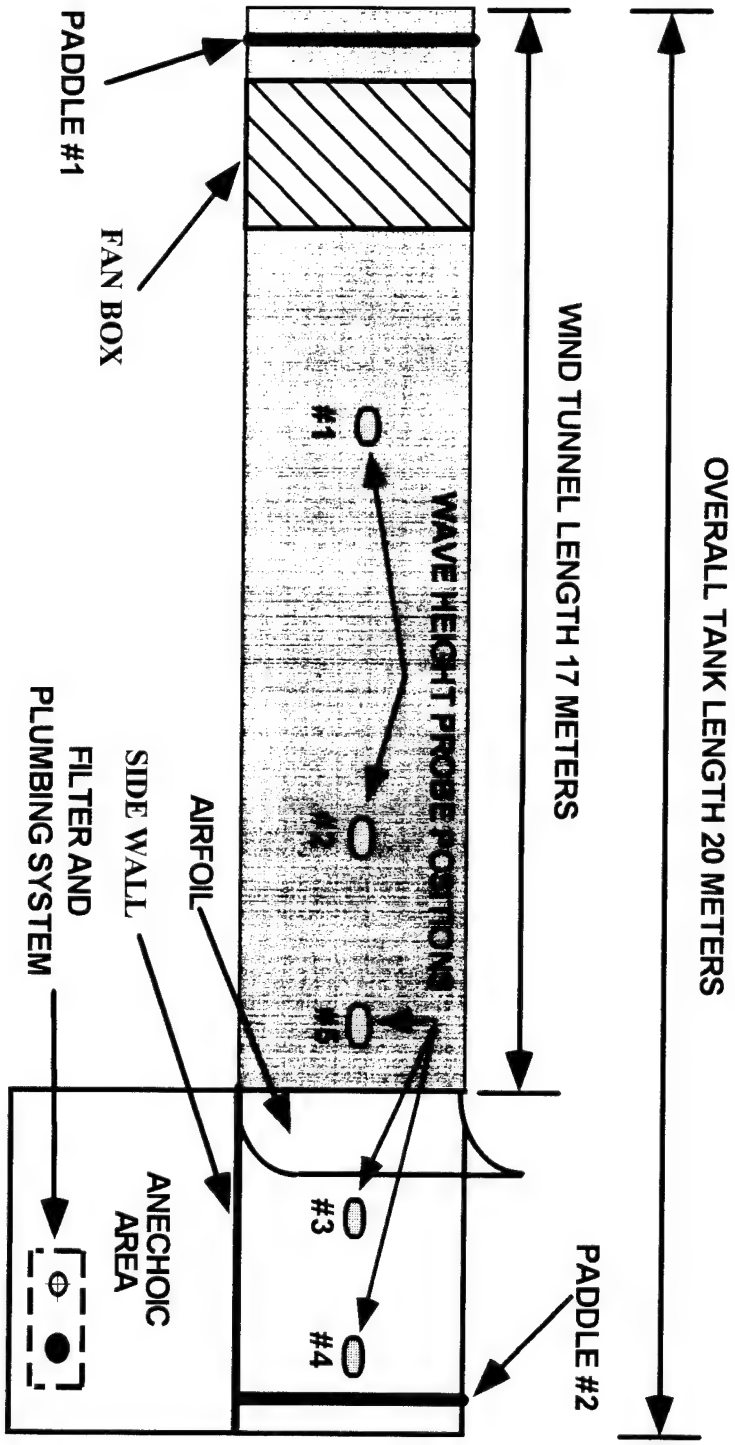

Figure 2-1. Wind -Wave Tank and Components.

C. WIND GENERATION

The wind source consists of five pairs of 3/4 horsepower centrifugal fans on the top of a 1.8 meter long, 1.0 meter wide, 1.0 meter high housing. The fans were reconfigured symmetrically and electrically switched in three groups with the first group consisting of a single fan pair, and the remaining two fan pairs consisting of two fans each as shown in Figure 2-2. The fans are mounted so that they discharge vertically down through a large wooden box (fan box). Baffles near the bottom of the box deflect the air stream horizontally as it exits the fan box, and creates a small impact area directly under the fan box. A relatively quiescent area remains between the fan box and the paddle.

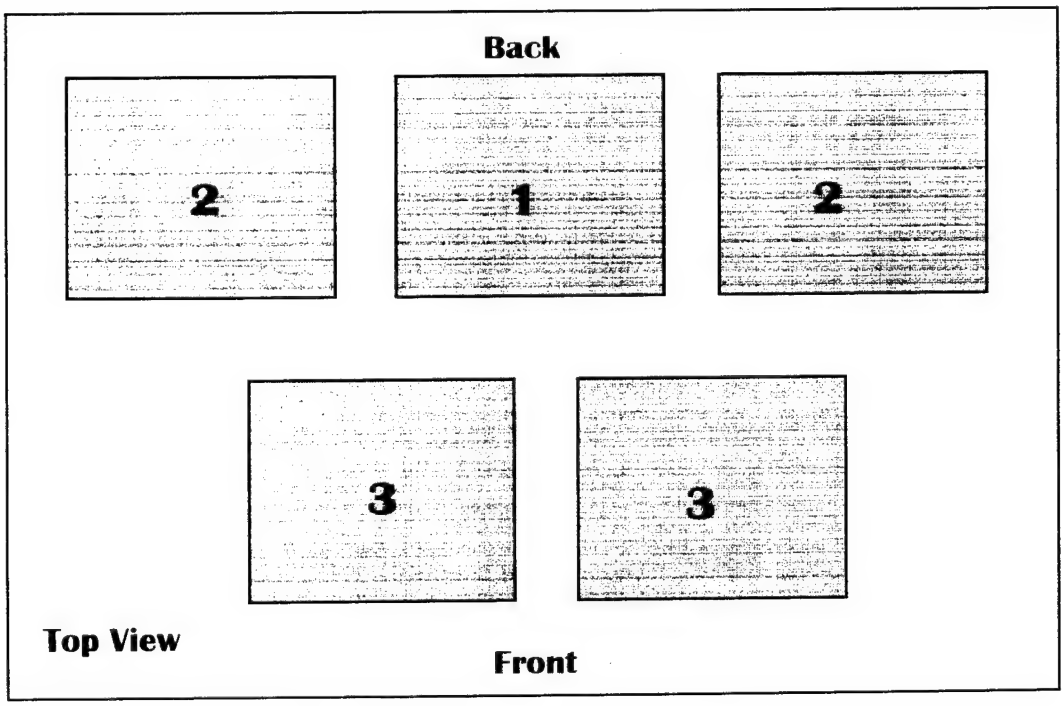

Figure 2-2. Fan box configuration.
Five pairs of 3/4 horsepower centrifugal fans located at one end of the tank. The fans are electrically switched in three groups with the first group consisting of a single fan pair, and the remaining two groups consisting of two fan pairs each.

Used in different combinations, a wide range of wind velocities can be obtained. The wind was measured before the airfoil and just inside the wind tunnel at approximately the center of the wind tunnel cross sectional area. Wind speed was measured using a hand held Turbo-meter^{TM} manufactured by Davis Instruments of San Leandro, CA. To insure maximum sensitivity and accuracy, the turbine is suspended on sapphire jewel bearings and its rotation is sensed by an infrared light beam, which adds no friction. The uncalibrated, measured wind speeds are reported in Table 2-1.

Fan Combinations	Wind Speed (m/s +/- .1)
F0	0.0
F1	1.6
F3	2.2
F1 & F3	2.9
F2	3.0
F2 & F3	3.8
F1 & F2	4.2
F1 & F2 & F3	5.0

Table 2-1. Measured Wind Speeds for various fan combinations.

D. THE PADDLES

There are two paddles configured on the tank. Paddle one is mounted on the same end as the fan box and paddle two is on the anechoic end of the tank. The paddles are the controllable source of waves and consist of a sheet of plywood just less than the width of the tank, .30 meters deep, and hinged on their bottom edge .05 meters below the water surface to a plywood structure in such a way as to form a box with a movable side. The box is surrounded by a rubber sheet, folded to allow free movement of the paddle, which keeps the space behind the paddle free of water. The top edges of the paddles were mechanically driven horizontally by linear motors, and the outgoing waves were directed down the tank. The motors, APS Models 113 and 400 Electro-SEIS Shaker respectively, manufactured by APS Dynamics, Inc. of Carlsbad, CA, were linked to the paddle with a 1/2 inch threaded rod with ball joints at both ends. In turn, the motors were electrically driven by APS Models 114 and 144 Power Amplifiers, which amplified the analog waveforms generated by computer. Because the waveforms were often broadband noise with occasional large excursions, a Surge Protector, Figure 2-3, was built and added between the power amplifier and Macintosh Quadra 900 computer to keep from blowing fuses in the amplifier and to protect the paddle from banging against the end of the tank when voltage spikes occurred.

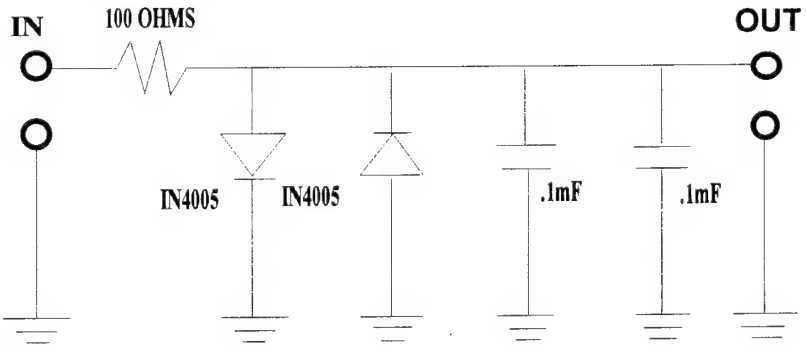

Figure 2-3. Surge Protector.
The Surge Protector was placed between the power amplifier and the computer to keep from blowing fuses in the amplifier and to protect the paddle from banging against the end of the tank.

E. WAVE HEIGHT PROBE

The sensing of water height by a four wire probe was addressed by Yarber (1992). Its output is an analog voltage signal proportional to the wave height. It operates on a lock-in amplifier principle using an external input AC signal as a carrier signal. The wave probe is placed vertically into the water so that the plane formed by the probe wires is perpendicular to the wave direction. The outer two wires are driven by alternating current sources of opposite polarity, and each of the two inner wires sense a voltage proportional to the complex impedance between them. A divider circuit converts the impedance signal into an admittance signal, which is proportional to the height of the water. A rough static calibration was performed and its sensitivity found to be 0.40 meters per Volt. Positive and negative fifteen volt DC power is supplied to the circuit by a Kepco MPS-60 Multiple Output Power Supply. The output of the circuit is carried by BNC cable to the Macintosh Quadra 900 computer where it is digitized. The external 10 kiloHertz 5 Volt Fixed Sine input signal from the HP3562A Dynamic Signal Analyzer is also carried by BNC cable.

The wires on the probe had to be re-soldered and epoxied during the course of this work due to lack of tension being maintained and they were also showing signs of corrosion or scaling which could have had adverse affects on the accuracy of the measurements. A mild sandpaper was carefully used to extract most of the build-up. New probes have been designed using an improved circuit. The idea is to be able to place numerous probes along the length of the tank enabling one to take measurements at different positions simultaneously vice having to move the probe to a new position prior to each series of runs.

Four probe positions were monitored for the burst propagation experiment. Two positions were located within the wind tunnel while the other two were located in the open part of the tank. These particular positions required two methods of insertion of the probe. For the positions inside the tunnel, because of a physical obstruction on top of the tank, it was necessary to "rig" the probe onto a small stick, Figure 2-4, and slide it in from the side with a clearance of about 10 centimeters and push it into a rectangular hole

the side with a clearance of about 10 centimeters and push it into a rectangular hole already cut in the top of the tank. For the positions in the open part of the tank, the probe was attached to a specially-made board laid across the water between the side walls of the tank.

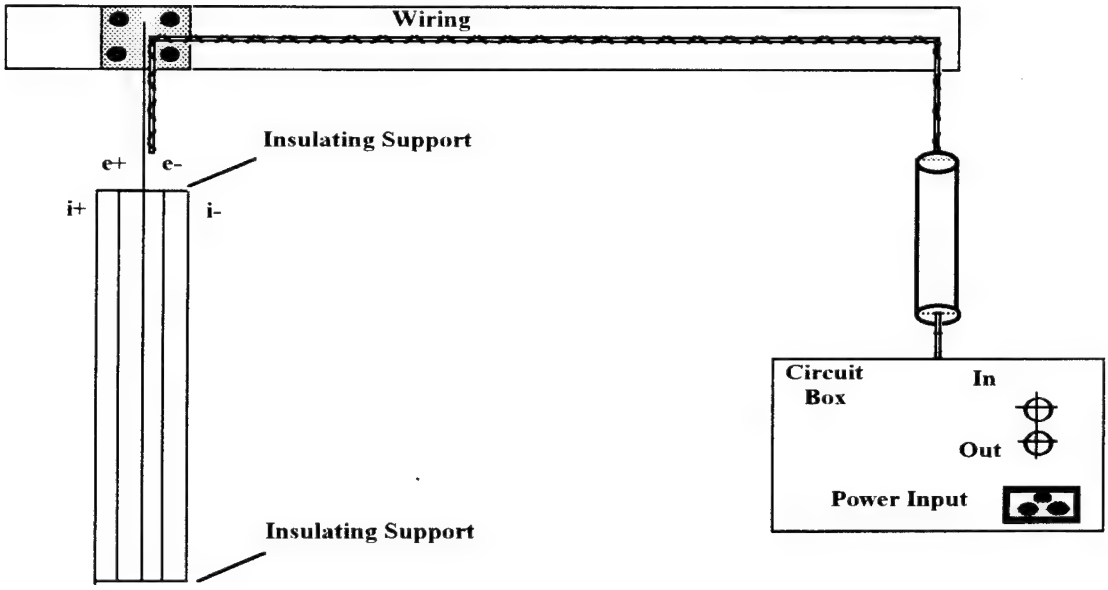

Figure 2-4. Four-wire probe (Yarber, 1992).
The four-wire probe specially "rigged" in order to access the probe positions located within the wind tunnel.

III. BURST PROPAGATION EXPERIMENT

A. DESCRIPTION

At the beginning of each run a new random broadband wave burst with cutoff frequencies of 1-3 Hz is launched by the upwind paddle number one. Simultaneously, a 102.4 second time record of the wave height at one of the four probe positions starts being collected. A Gabor spectrogram, giving the frequency content of the time record as a function of time, is then calculated. The program then waits 102.4 seconds plus an additional random time ranging from zero to 102.4 seconds to enable the burst to die out. This process is repeated 200 times; fewer times for the data taken with no wind. The spectrograms from each run are accumulated, averaged together, and displayed, and then stored after the series of runs is complete. The order in which the data is presented is based on wind speed and wave probe position. There were eight wind speeds used varying from 0 m/s to 5 m/s over four different transducer positions. As shown in the tank diagram, Figure 2-1, wave probe positions were at approximately 5 meters, 10 meters, 17 meters, and 19 meters, respectively. The most usable form of displayed data was a color image. By examining plots of spectral density, represented by color, versus time and frequency as shown in Figures 3-1 through 3-8, a distinction between the input burst and the effect due to the suspected collective mode can be made. Additionally, contour lines were used in combination with the color presentation and are helpful in determining particular characteristics of the image.

B. COMPUTER

A Macintosh Quadra 900 computer running LabVIEW 3.0 (1993) controlled the experiment. Four main program panels, three of which were developed by Lawrence (1992), were utilized in running the various experiments. The Waveturb Virtual Instrument is the main program which showed the data as it was averaged after each run. The Burst Generator front panel allowed one to control the paddles with a specific waveform. The Gabor spectrum, allowed one to look at the Waveturb 1.4 data in terms

of a frequency versus time display and the Data Acquisition Virtual Instrument panel allows the number of samples as well as the sampling frequency to be controlled. Parameters and block diagrams were modified slightly from Lawrence's work. Each run was saved in LabVIEW as an ASCII formatted file named by the operator. Once saved, the data was converted to log data and further processed and displayed using SPYGLASS™ et al. (SPYGLASS™ Transform, 1993 and Format, 1991).

The Burst generator panel mentioned earlier serves as the primary driver of the paddles. It is designed so that various forms of wave burst can be generated from narrowband to broadband over a range of frequency intervals. If a noise burst is used, cutoff frequencies of a bandpass filter and duration of the burst can be chosen, whereas for a sine wave burst, the frequency, amplitude, and the duration of the pulse are specified. The burst envelope can also be varied in order to smooth the reaction of the paddle at beginning and ending edges of the burst. The burst envelope used for this experiment was a ten-percent tapered noise burst with cutoff frequencies of 1-3 Hertz. As Lawrence (1992) explained, wave height data is sampled immediately following each launch of a wave pulse. The analog signal from the probe electronics is converted to a 16 bit digital signal and sampled at a 20 Hz frequency sampling rate by a National Instruments NB-MIO16XL board inside the computer.

C. RESULTS AND INTERPRETATION

Figure 3-1 shows the burst only with no wind over the four positions starting with the 5 meter data at the top. As the probe is moved further and further away from the paddle producing the burst, it can be seen that the burst spreads out due to slower propagation speeds at the higher frequencies. As was described earlier, linear gravity waves have an arrival time proportional to frequency, stretching the burst energy along a diagonal swath on the spectrogram. Also visible at frequencies just above one Hertz are the reflections of energy from the far wall. Beginning with the slowest fan speed combination, we see in Figure 3-2 an interesting feature, a decrease in energy immediately after the burst. This area of energy depletion may be related to the collective mode. The

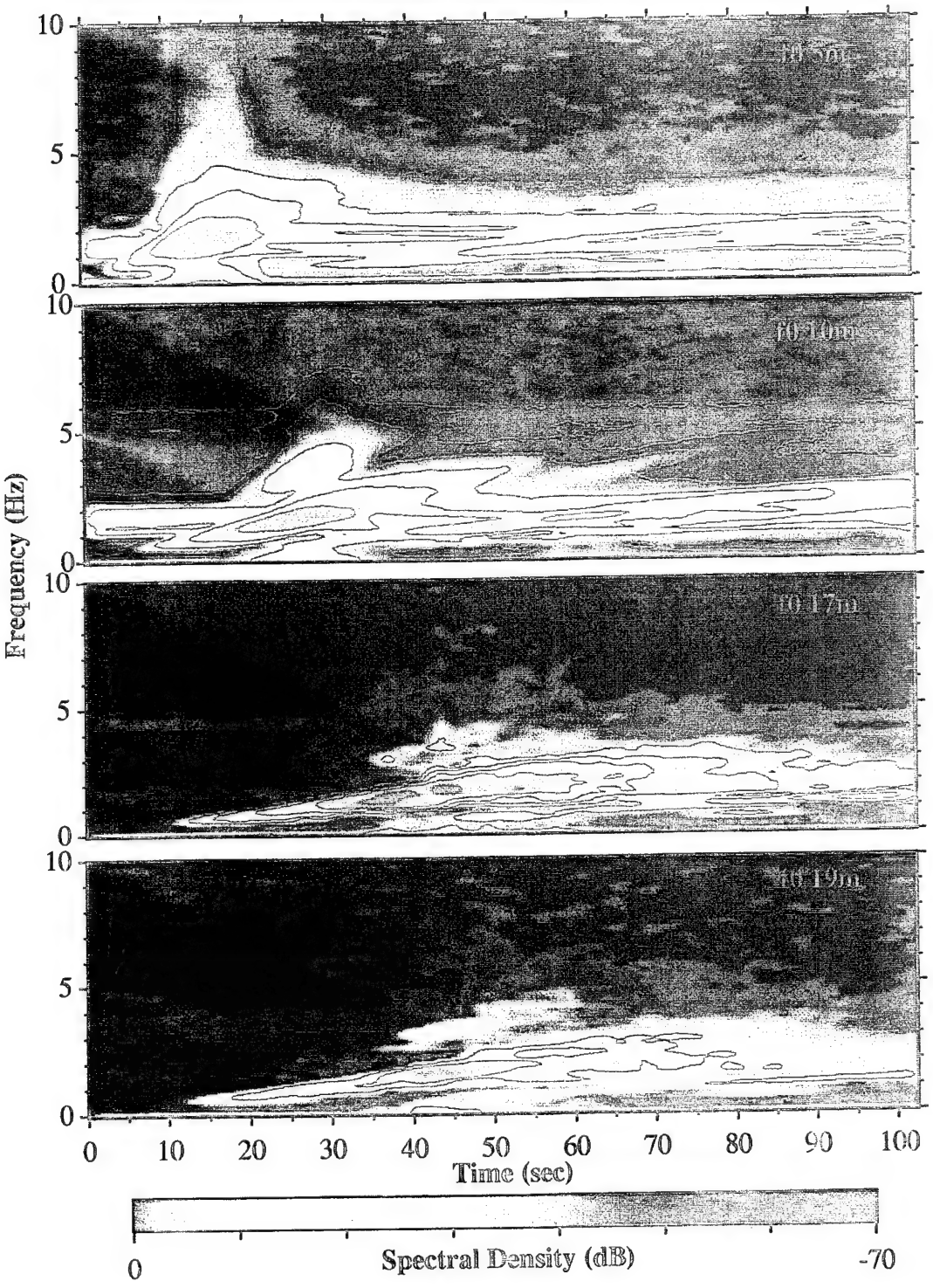

Figure 3-1. Wind-Wave Tank Plot for a 0.0 m/s Fan Speed at Probe Positions of 5m, 10m, 17m, and 19m.

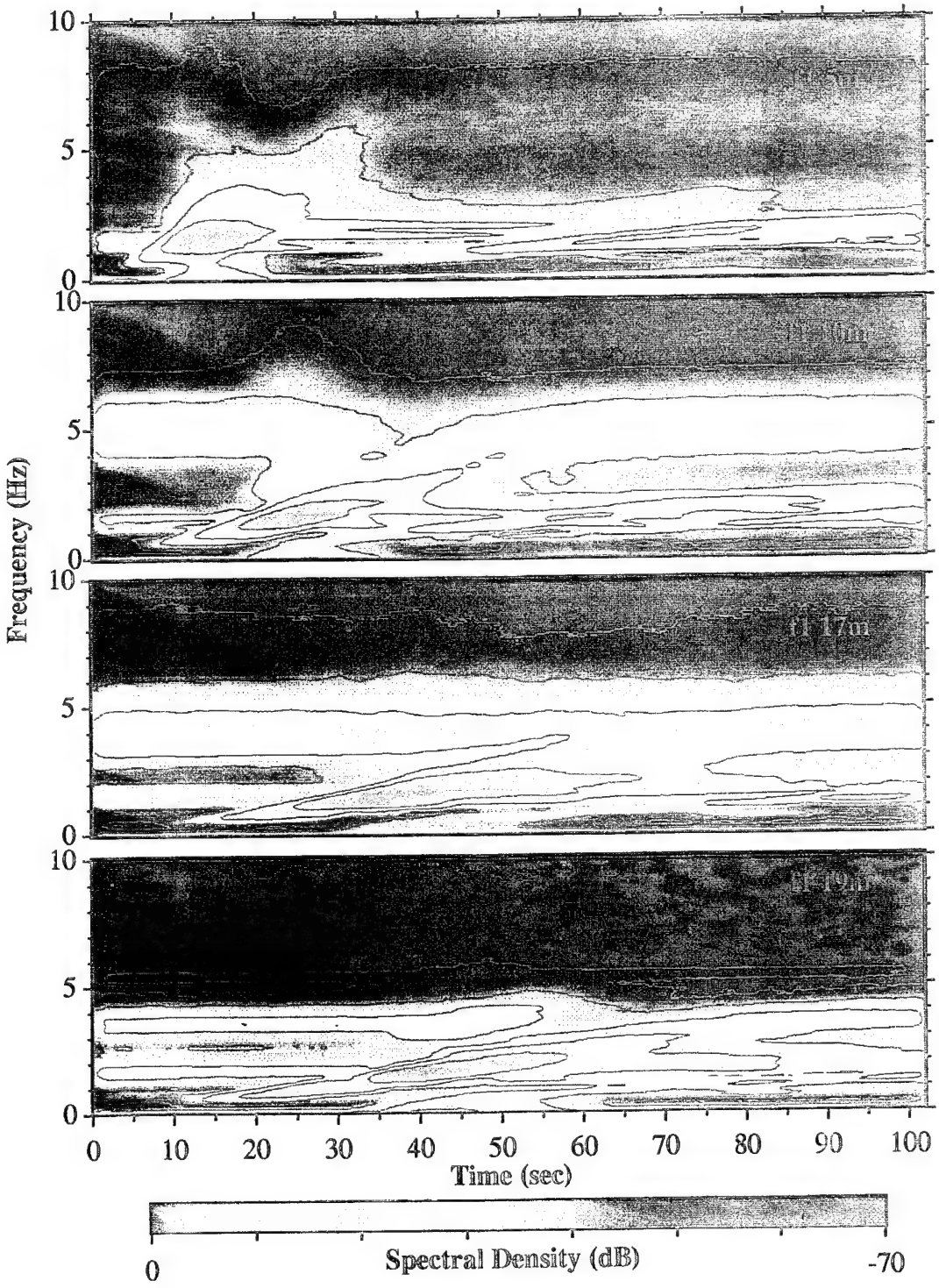

Figure 3-2. Wind-Wave Tank Plot for a 1.6 m/s Fan Speed at Probe Positions of 5m, 10m, 17m, and 19m.

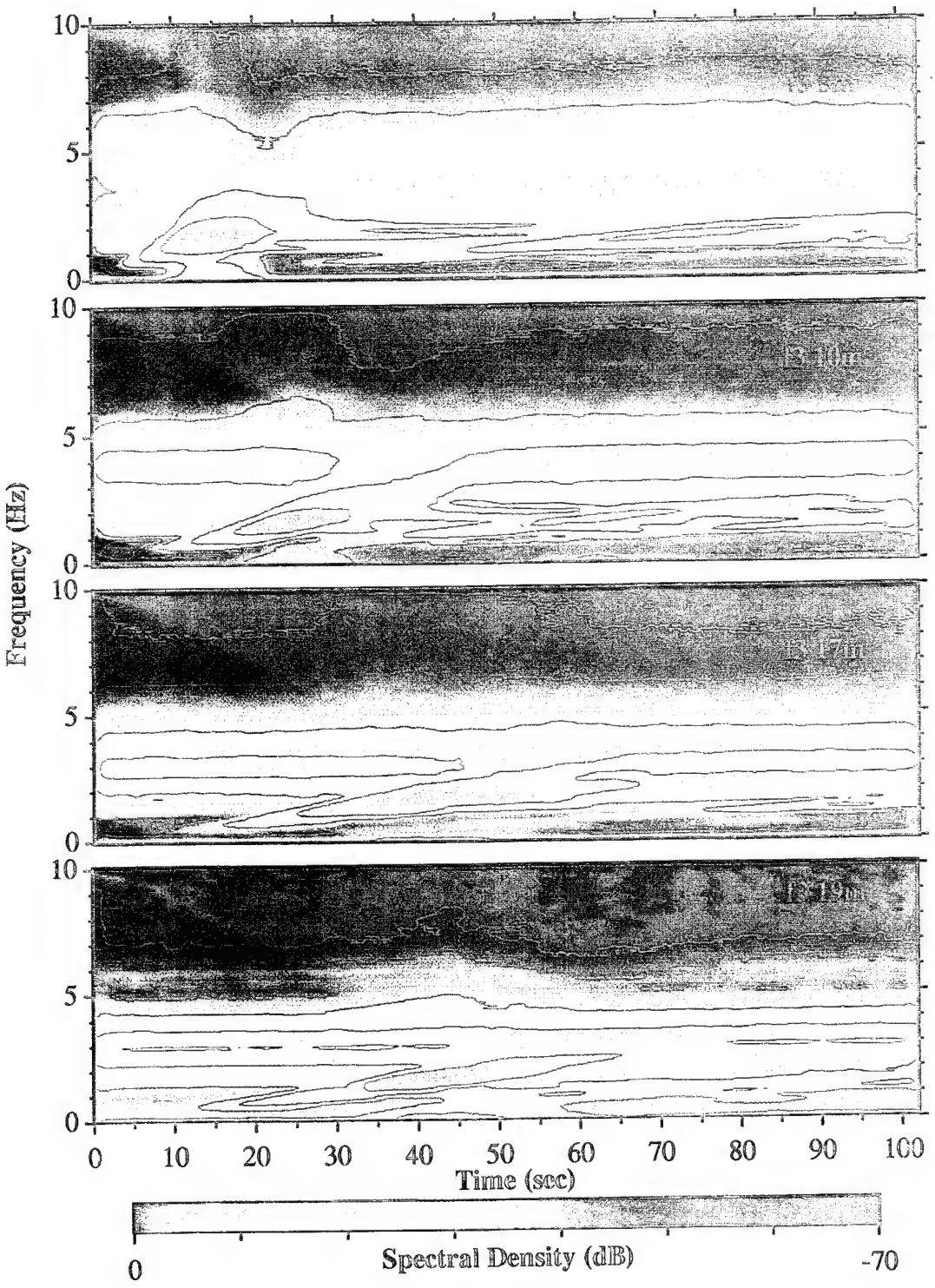

Figure 3-3. Wind-Wave Tank Plot for a 2.2 m/s Fan Speed at Probe Positions of 5m, 10m, 17m, and 19m.

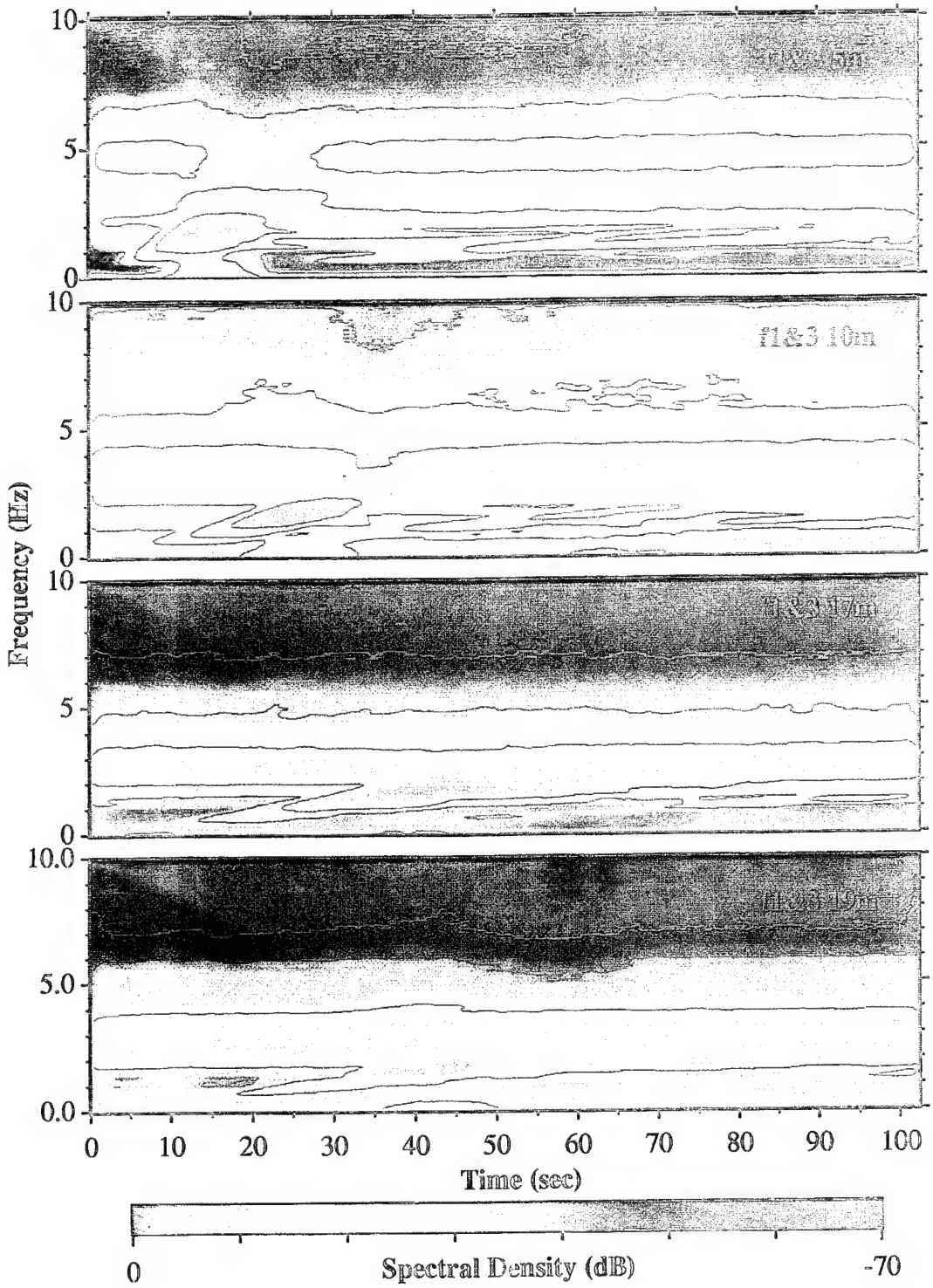

Figure 3-4. Wind-Wave Tank Plot for a 2.9 m/s Fan Speed at Probe Positions of 5m, 10m, 17m, and 19m.

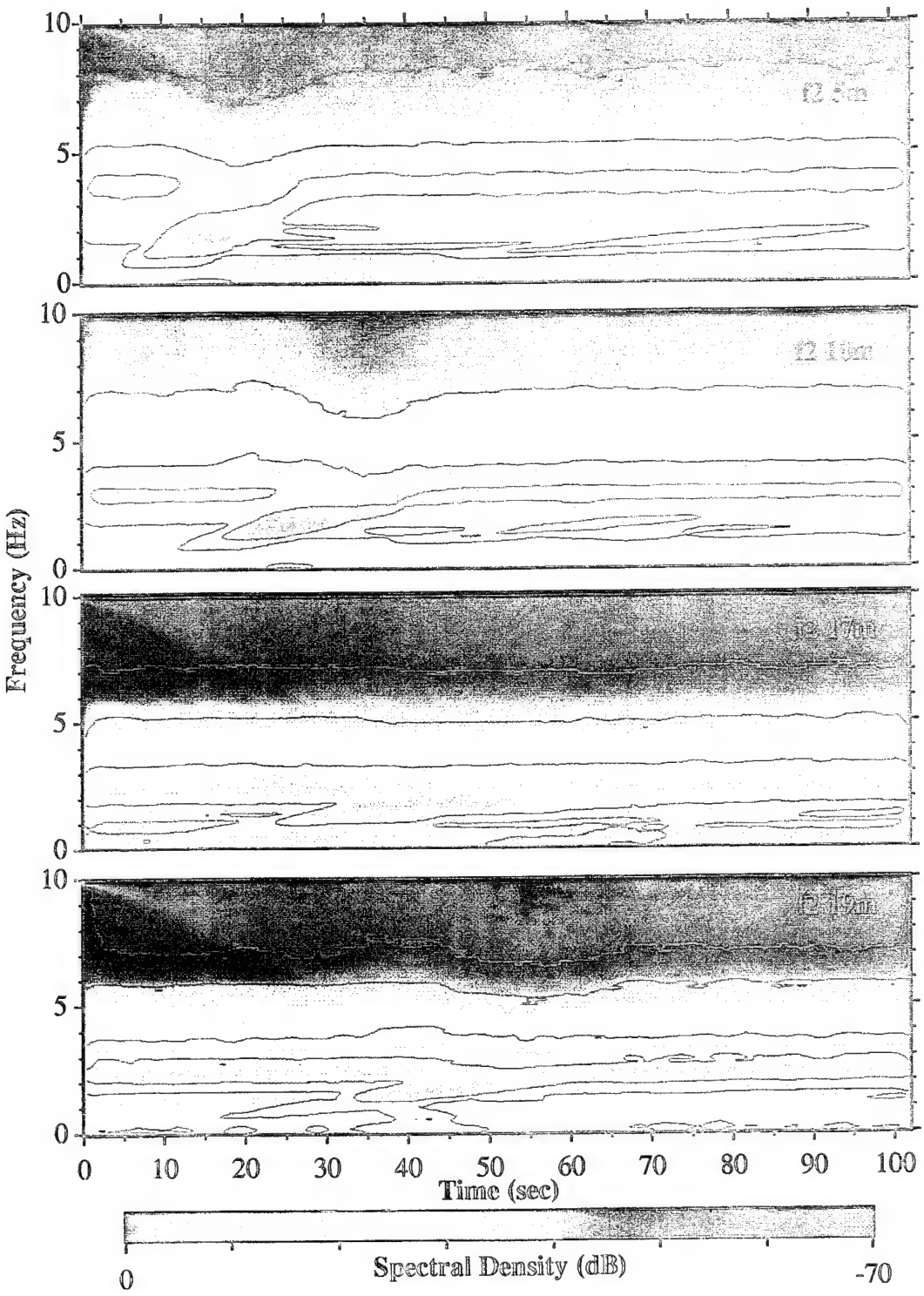

Figure 3-5. Wind-Wave Tank Plot for a 3.0 m/s Fan Speed at Probe Positions of 5m, 10m, 17m, and 19m.

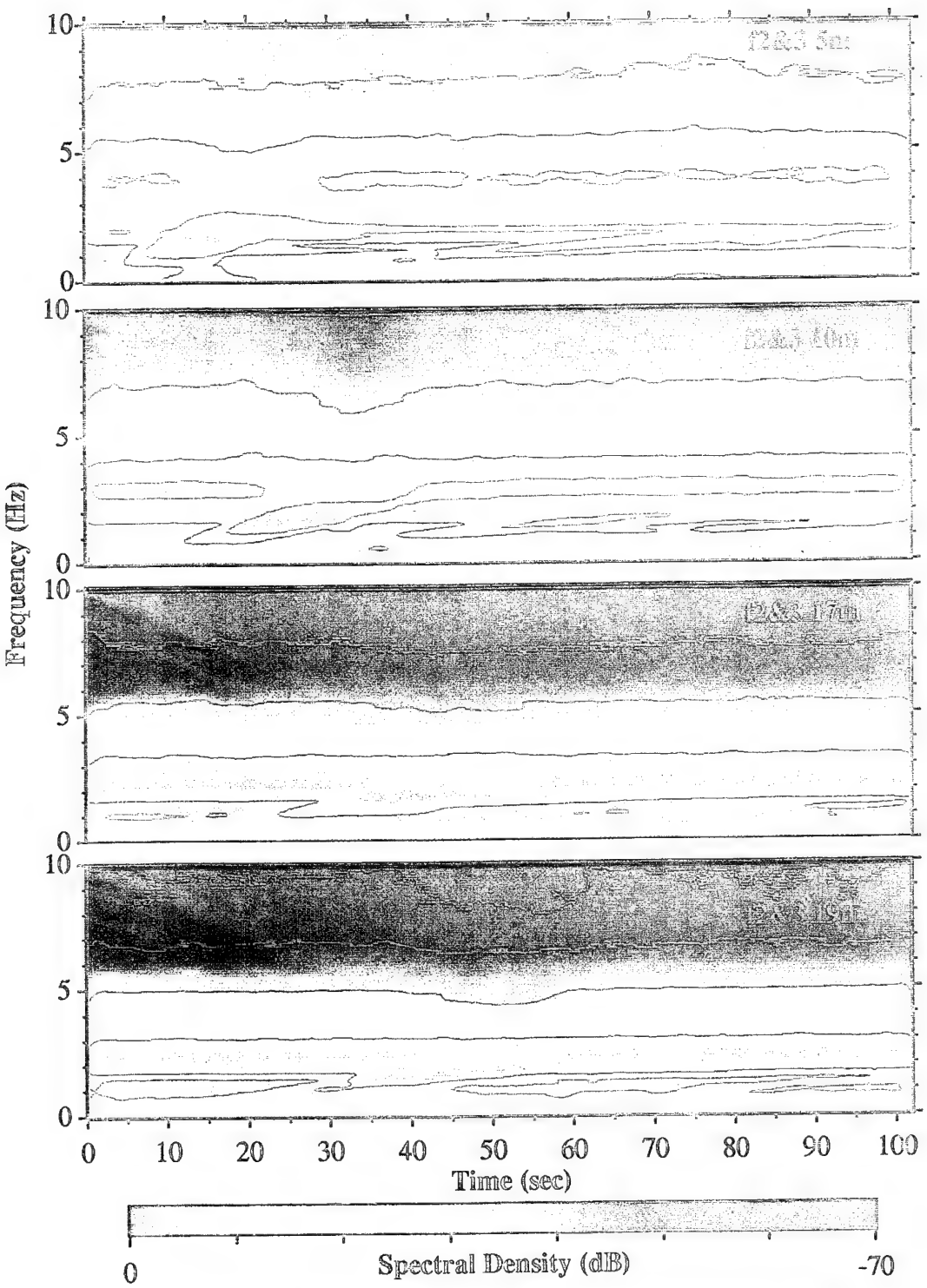

Figure 3-6. Wind-Wave Tank Plot for a 3.8 m/s Fan Speed at Probe Positions of 5m, 10m, 17m, and 19m.

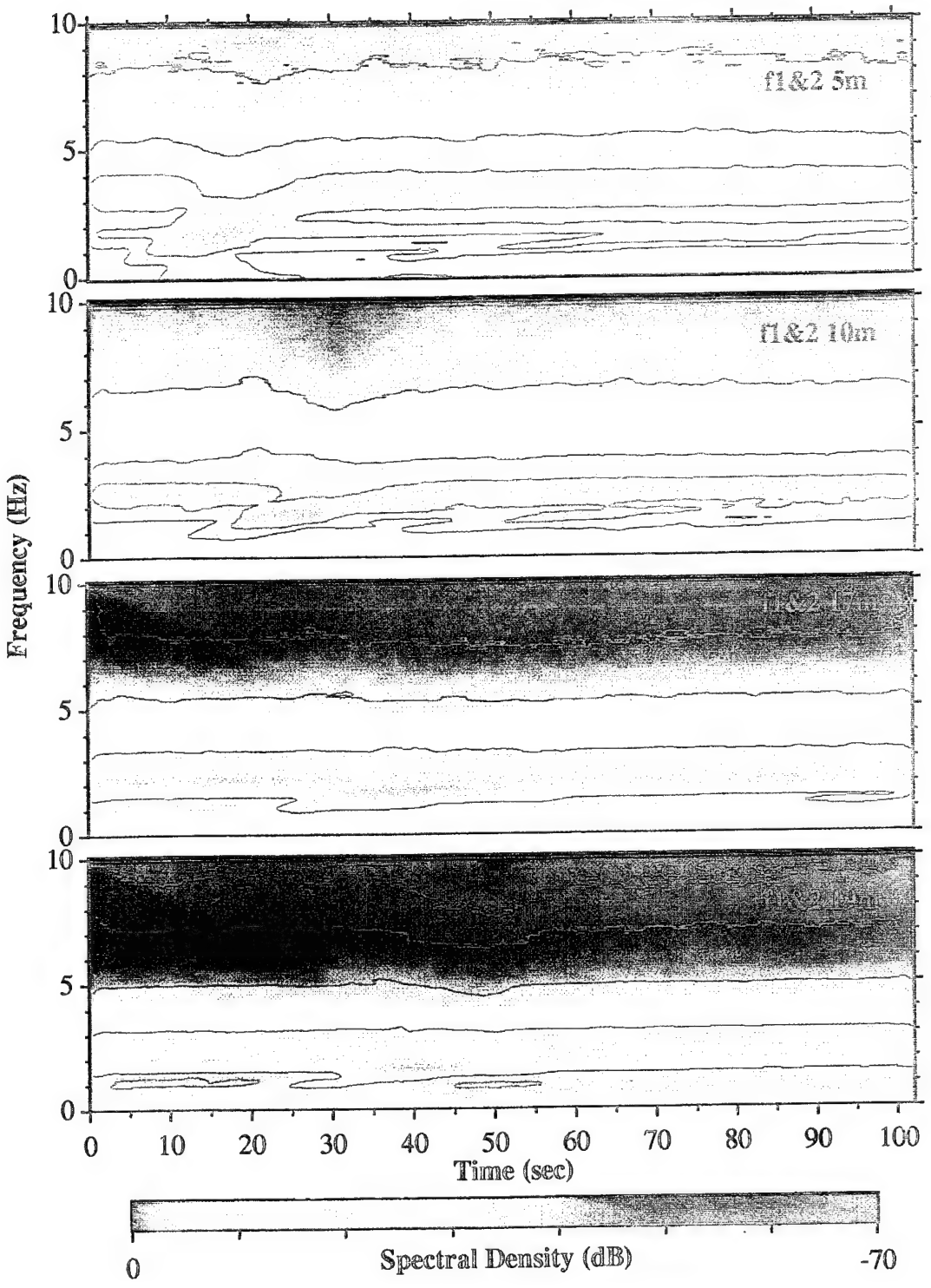

Figure 3-7. Wind-Wave Tank Plot for a 4.2 m/s Fan Speed at Probe Positions of 5m, 10m, 17m, and 19m.

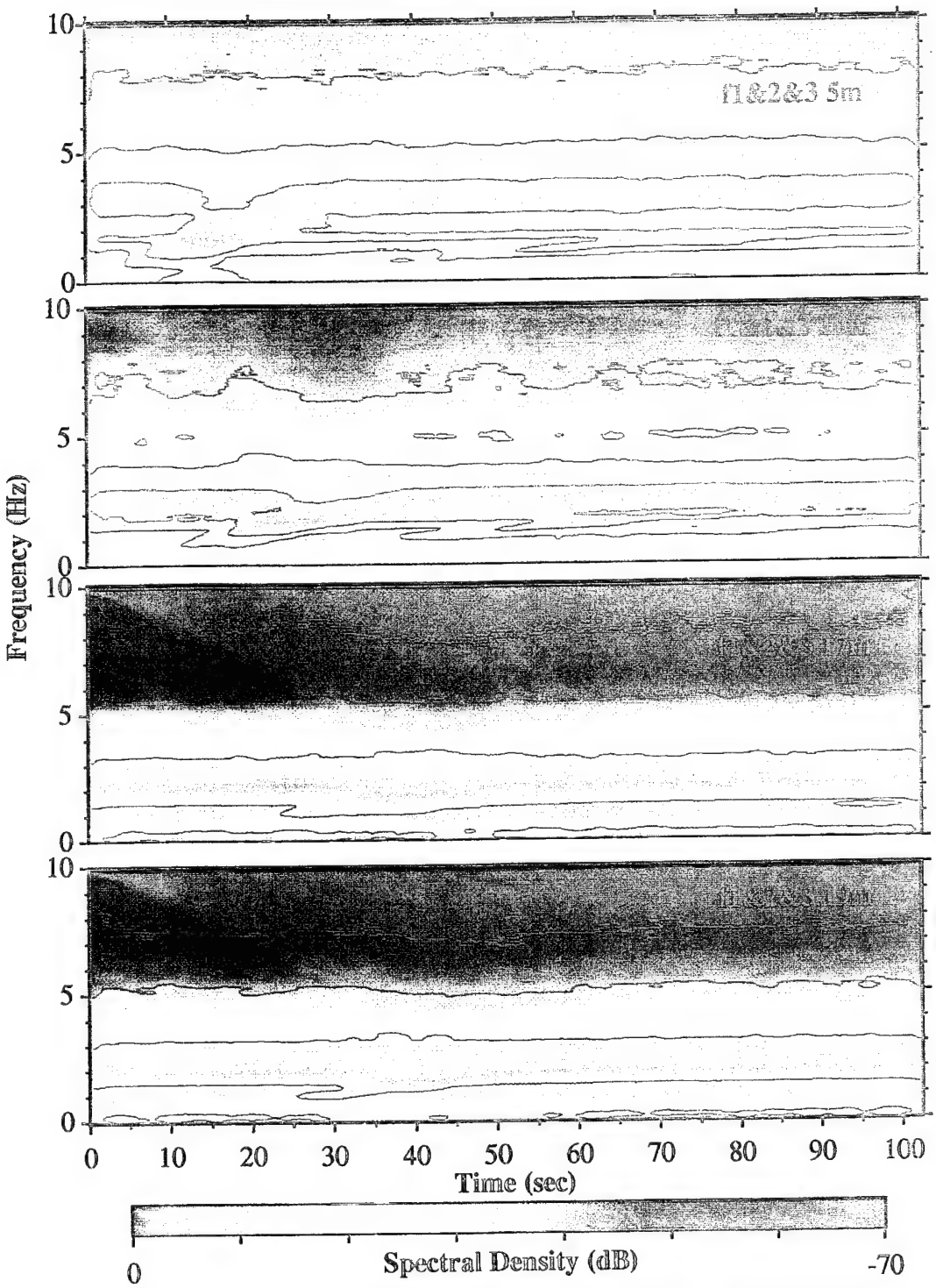

Figure 3-8. Wind-Wave Tank Plot for a 5.0 m/s Fan Speed at Probe Positions of 5m, 10m, 17m, and 19m.

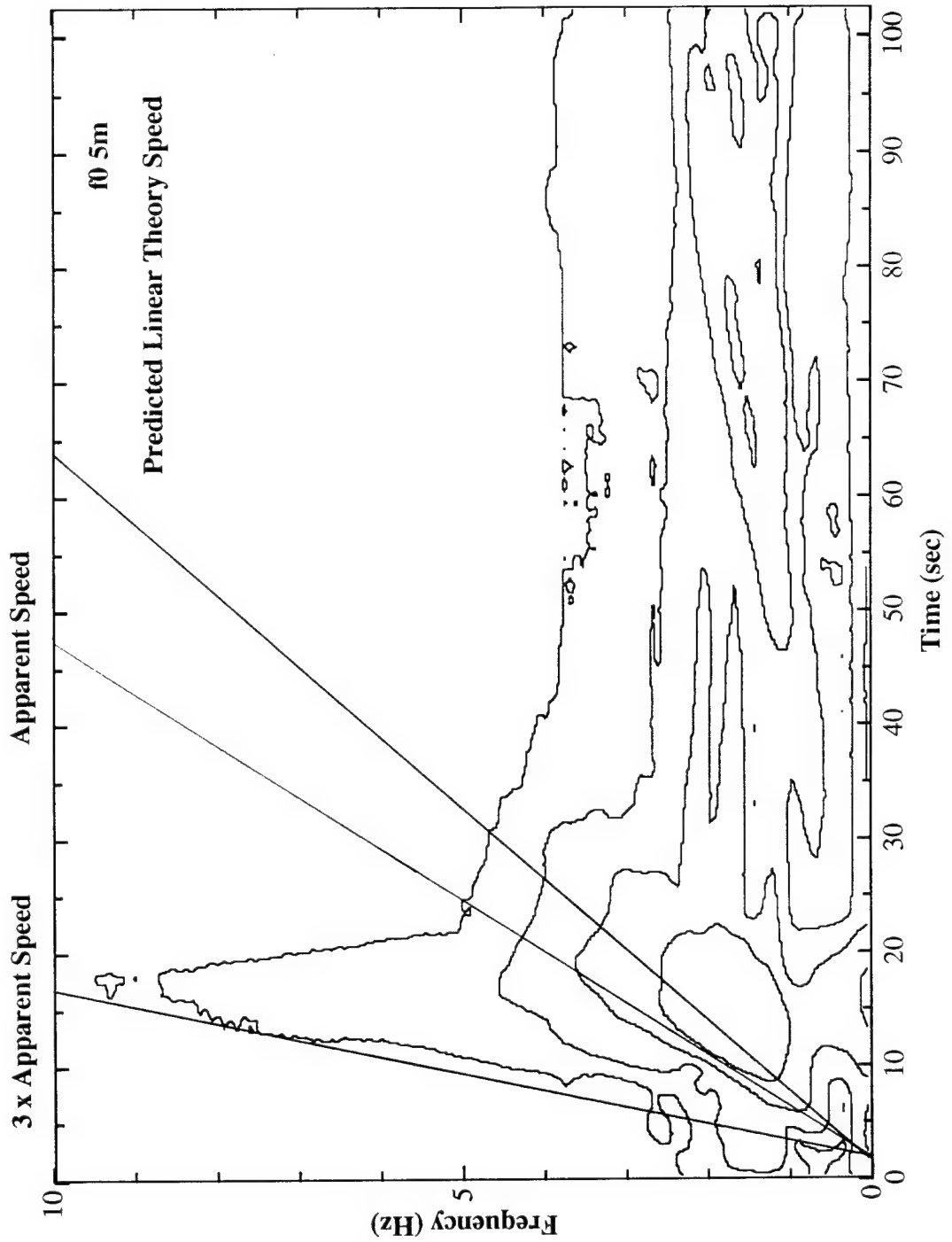

Figure 3-9. Wind-Wave Tank Data showing the characteristics of the velocities based on the frequency components of the burst. The lines do not cross at the origin due to a delay encountered at the paddle at input.

IV. MODE COUPLING EXPERIMENT

A. DESCRIPTION

While running the burst propagation experiment, it was occasionally observed that the fundamental mode of the tank was somehow excited and this excitation was modulating the intensity of the wind generated background. It was realized that this amplitude modulation of broadband background is another way the collective mode could assert itself. In the following experiments, the fundamental mode of the tank was driven by one of the paddles to act as a long, low frequency wave, called the "swell". The fluid velocity associated with the swell should convect along any short waves generated by wind, called the "chop", riding on top of the swell. If the chop waves did not interact, it would be expected that they should accumulate where swell has accumulated the most water, which would be at the crest of the swell. However, since the gravity waves propagate more quickly, as can be seen from the dispersion relations plotted earlier in Figure 1-1, they drive the collective mode above the collective mode resonance frequency, and like a pendulum driven above its resonance frequency, the collective mode should lag the gravity waves in its response due to collective "inertia" of the background of waves. Further description can be found in Davies (1994).

Using Davies' (1994) techniques, it was possible to separate swell and chop components with filtering, and to compute and relate both the instantaneous amplitude of the chop to the instantaneous phase of the swell using the Hilbert Transform. In the time domain, Figure 4-1a shows, for example, the original unfiltered tank data for a 3.0 m/s wind speed and transducer position of 17 meters. By using low pass and high pass Chebyshev Type II filters, the low frequency swell could be separated from the high frequency chop, Figures 4-1b and 4-1c respectively. Figure 4-2 shows the power spectra of these three waves and illustrates how they relate to each other in the frequency domain. To capture the swell frequency, the low pass cutoff frequency was set at 0.2 Hz, while, to separate out the chop, the high frequency cutoff was set at 1.5 Hz.

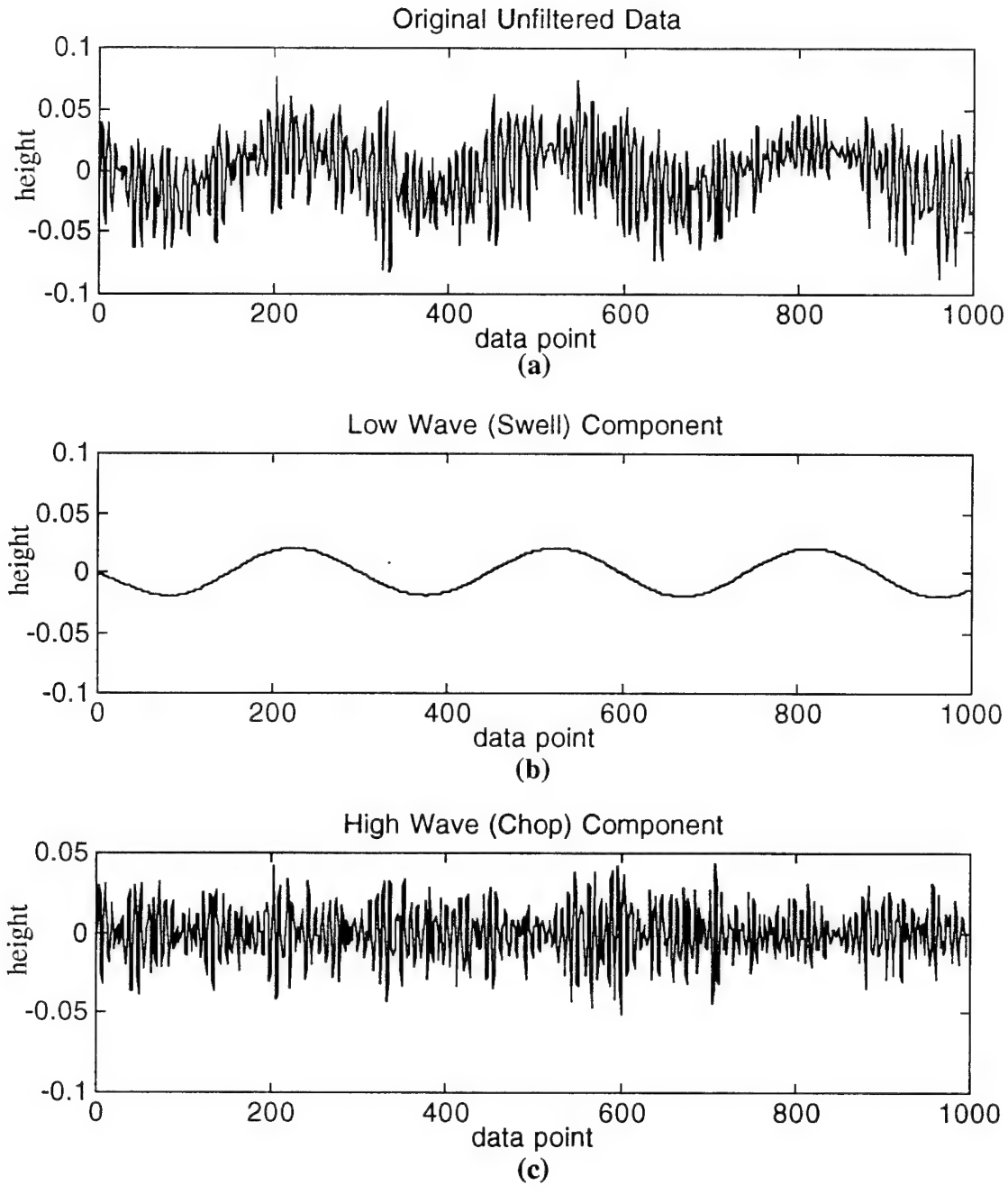

Figure 4-1. The Chop and Swell Components produced by the Low and High Pass Filters in Davies (1994) Filtering Program. Swell is the output of the Low Pass filter. Chop is the output of the High Pass filter. Data shown for wind speed of 3.0 m/s and transducer position of 17 m.

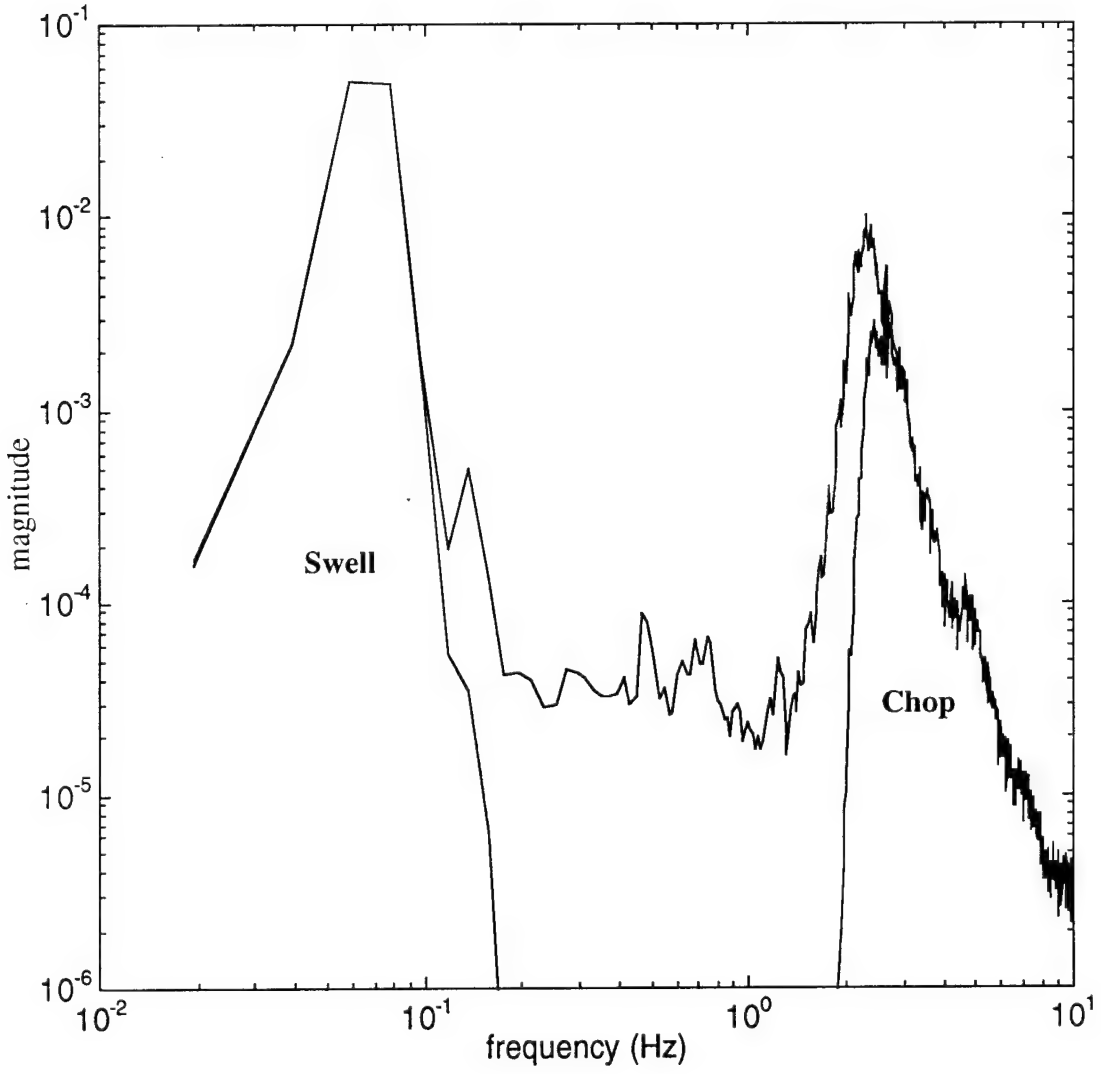

Figure 4-2. Power Spectra relationship of the Swell and Chop of the Wind-Wave Tank at a wind speed of 3.0 m/s and transducer position of 17 m. Cutoff frequency for the swell is 0.2 Hz. Cutoff frequency for the chop is 1.5 Hz.

B. THE FUNDAMENTAL MODE

There were two methods used to determine the optimal driving frequency for the fundamental mode of the tank. A power spectrum was first taken using a 1 Hz span display on a Hewlett 3562A Dynamic Signal Analyzer with 200 averages while wind slightly excited the lowest mode of the tank. This allowed us to identify a "ballpark" figure for the fundamental frequency. To determine the accuracy required, it was necessary to calculate the quality factor or "Q of the tank." The Q measured for the tank was

$$Q = \pi\left(\#\text{ cycles to decay by } e^{-1}\right) = 90. \tag{4.1}$$

Therefore, because the Q of the tank was so high, the frequency needed to be "fine tuned" to within one percent. To do this a free decay method was used.

First, with no wind in the tank, the approximate fundamental mode was driven by the paddle. Once the mode was built-up, as verified by observing water movement in the tank and by observing the sine wave on a modified Waveturb 1.4 LabVIEW panel, the paddle was shut off, and simultaneously the modified LabVIEW program was started. The modified Waveturb 1.4 panel does not include the Gabor Spectrum and allows long records of data to be collected in one run. Using 2048 counts and expanding the data over a sufficient amount of time, the free decay could be viewed.

From this, by counting the number of cycles for a specific time period, the Period of the mode could be calculated. Since

$$T = \frac{\Delta t}{\#cycles}, \tag{4.2}$$

where T is the Period of the mode, the frequency could be calculated using the relationship:

$$f = \frac{1}{T}. \tag{4.3}$$

Using the above calculated frequency as the new fundamental mode, the process was repeated until the frequency change was insignificant. In this case, only two runs were required to achieve a fundamental frequency of .06737 Hz.

C. MODULATION OF CHOP VERSUS PHASE OF THE SWELL

A sequence of wave height measurements containing 32,768 measurements taken at a 20 Hz sampling rate were made in the Ocean Acoustic Wave Facility. Paddle #2 in Figure 2-1 was used to excite the lowest normal mode of the tank, as discussed in the previous section, to simulate a swell. Then, a high frequency chop was generated by wind from fans blowing across the surface of the water in the tank. At first, it was our intent to expand a previous experiment run made for Davies to include not only the same observation of modulation of chop versus phase of swell for the fundamental mode but for higher modes of the tank as well. However, results for the fundamental mode were surprising in that different wind speeds and probe positions produced phase shifts that were not expected by the collective mode picture. Not fully understanding the physics going on in the tank, our efforts turned to documenting what was observed for the fundamental mode.

Originally, using an "un-tuned" frequency of .068 Hz, a Fan Two wind speed and a probe position of 17 meters, data analyzed by Davies provided strong evidence that indeed the collective mode, represented by the modulation of the chop, was being driven above its natural frequency of oscillation by the swell. Figure 4-3 shows the distribution plot of the amplitude of the chop, on the abscissa, versus the phase of the swell, on the ordinate. The phase values in the plot are shown in radians which represents the values $-\pi$ to $+\pi$. Specifically, phase values of zero represent the crests of the swell, the extremes represent the troughs of the swell, while $-\pi/2$ and $+\pi/2$ represent the falling and rising edge of the swell respectively. From this interpretation, the phase of the swell which achieves the maximum amplitude of the chop can be seen. For every particular phase of swell, the RMS average of the chop amplitude is shown as a solid line on the distribution plot. This

distribution plot that provided the strong evidence of the collective mode, Figure 4-3, showed that the modulation of the chop lagged the swell by 180° as expected by the collective mode picture. However, when this experiment was repeated with the "tuned" frequency and the probe at 19 meters vice 17 meters, the opposite occurred. A 0° phase shift was observed, Figure 4-4. Repeating the original set-up with the "un-tuned" frequency, the probe at 17 meters, and Fan #2 providing the background spectra, results were similar to those shown in Davies' thesis. To ensure an inversion of the measurements had not occurred, a sign test experiment, explained in Appendix A, was conducted. The sign test was the same as that performed for Davies on the original data. The experiment again showed that an inversion error had not occurred. Therefore, probe position became our primary focus.

To ensure that the distribution plots were not showing a phenomenon related to reflection off the far end of the tank and to help clarify the physics, a new probe position at 15 meters, labeled as #5 in Figure 2-1, was chosen. In addition, further study of various wind speeds revealed changes in the distribution plots. The wind speeds chosen were low (Fan 1 at 1.6 m/s), medium (Fan 2 at 3.0 m/s), and high (Fan 1&2&3 at 5 m/s) for probe positions of 10 meters, 15 meters, 17 meters, and 19 meters. Figures 4-5 through 4-7 represent the distribution plots for these various wind speeds and probe positions within the tank. The most interesting features are the double humps in Figure 4-5 at 19 meters and their apparent asymmetry in phase. The humps appear slightly to the right of $-\pi/2$, the trailing edge, and to the left of $+\pi/2$, the leading edge of the swell, both of which are toward the crest of the swell. Thus far, this phenomenon has not been explained. Also, in Figure 4-6 at 17 meters and 19 meters, the peaks of the phase are again asymmetrical in shape and almost seem to be propagating down the tank.

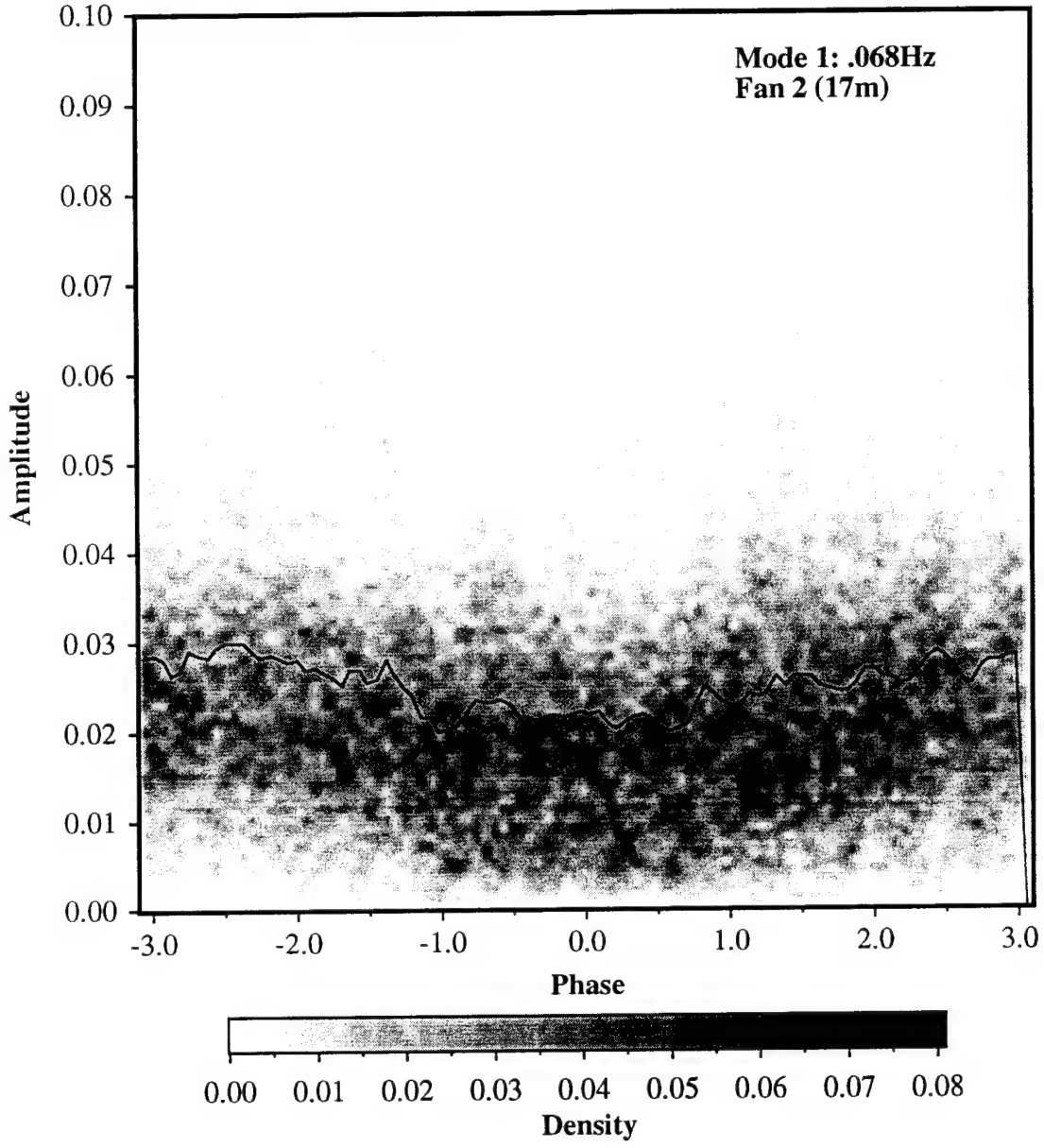

Figure 4-3. Distribution Plot of Amplitude of chop vs Phase of swell of the original data provided to Davies (1994). The solid line is the RMS amplitude of the chop. Two maxima are observed in the plot with a 180 degree phase shift between the amplitude of the chop and the phase of the swell.

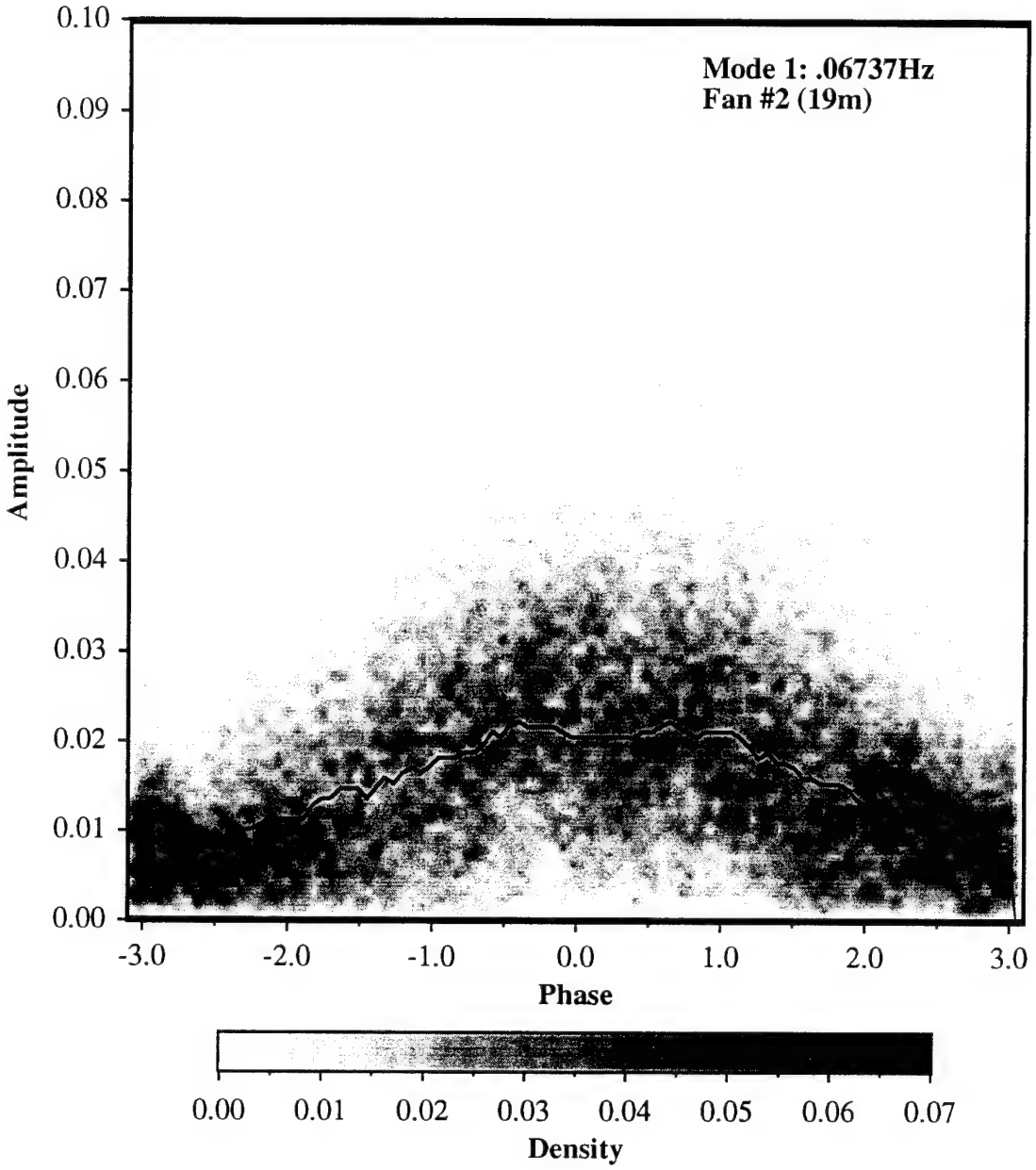

Figure 4-4. Distribution Plot of Amplitude of chop vs Phase of swell of data taken at the "tuned" frequency. The solid line is the RMS amplitude of the chop. One maximum is observed in the plot around a 0 degree phase shift between the amplitude of the chop and the phase of the swell. Notice it is not symmetrical in shape.

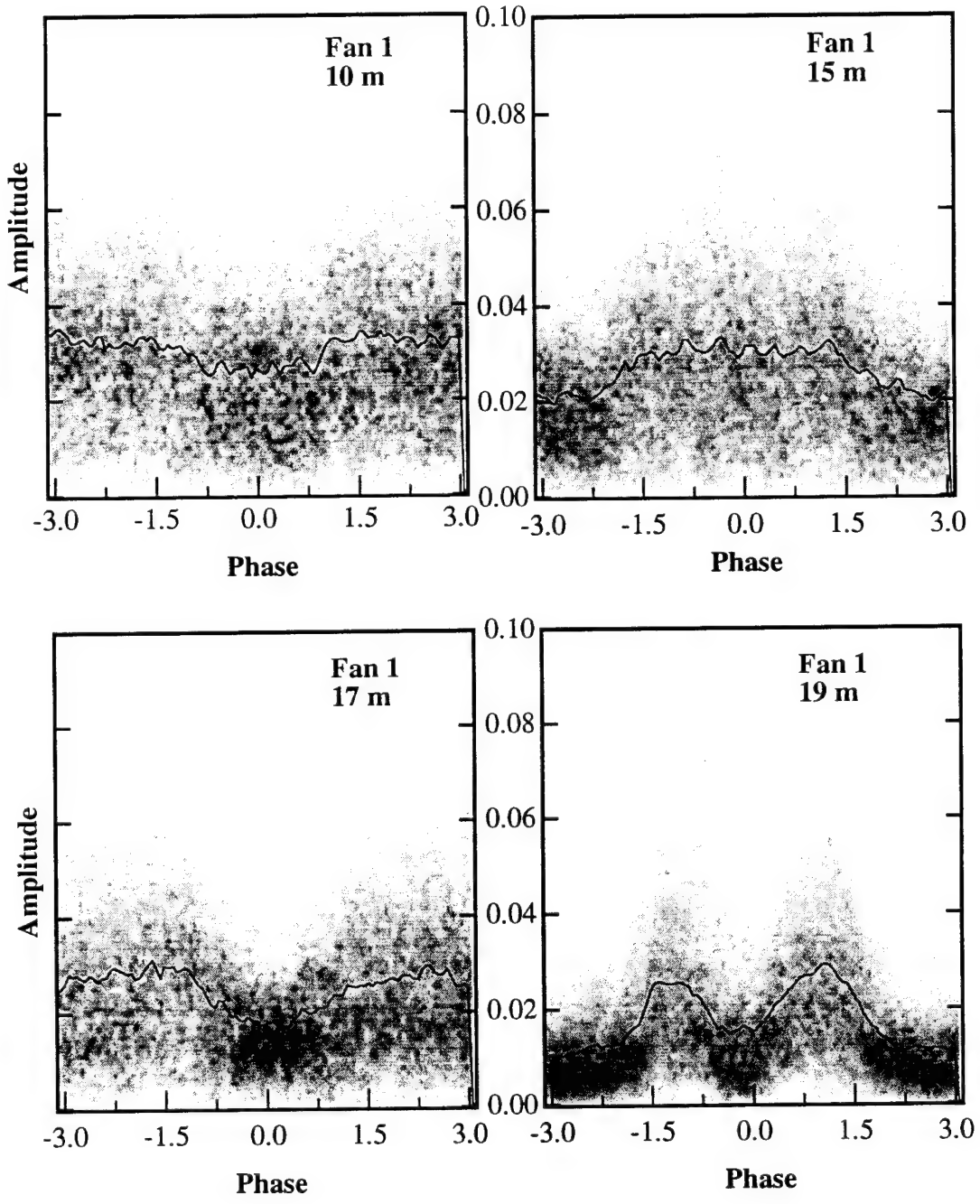

Figure 4-5. Distribution Plots of Amplitude of chop vs Phase of swell for a wind speed of 1.6 m/s at four different probe positions within the tank.

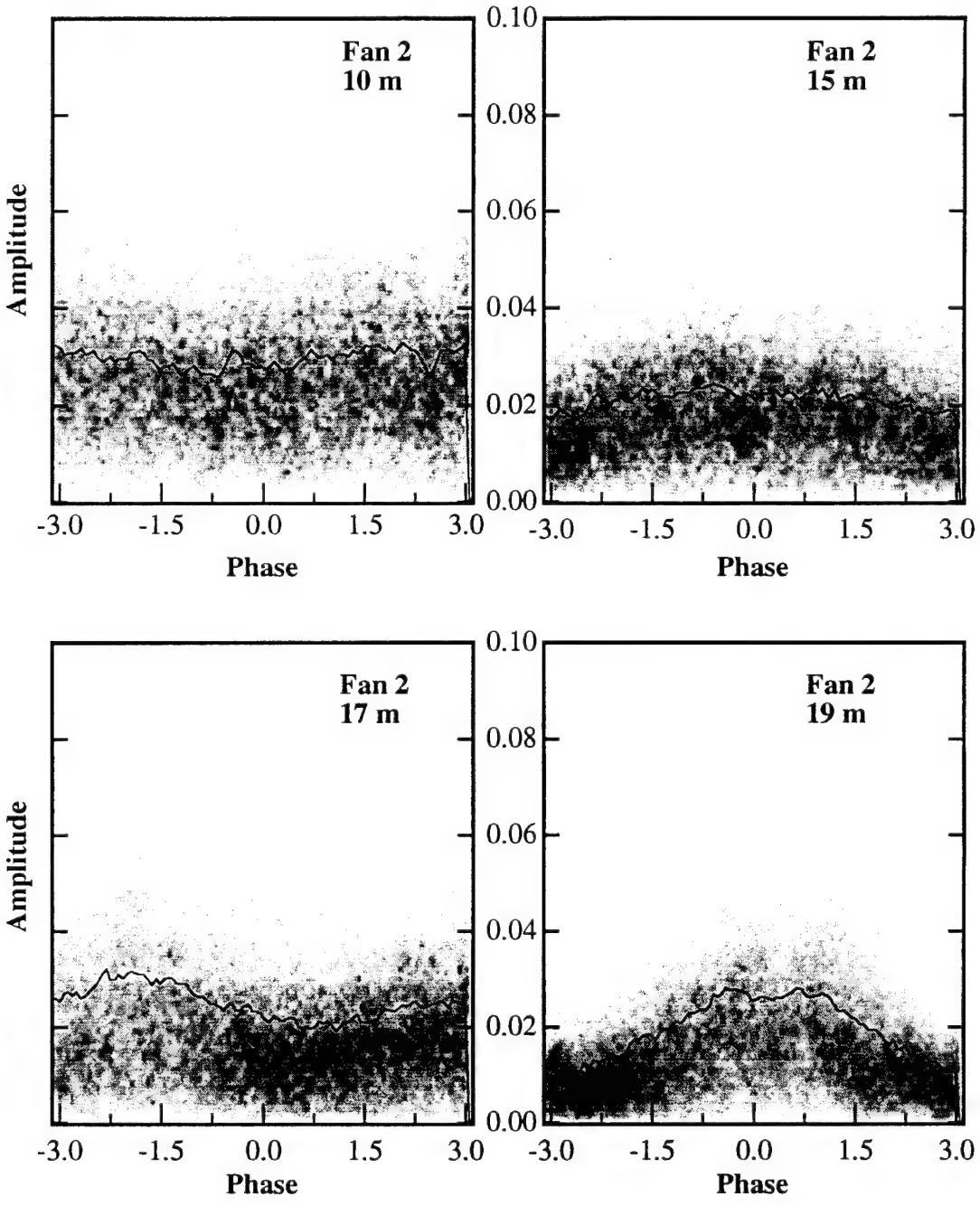

Figure 4-6. Distribution Plots of Amplitude of chop vs Phase of swell for a wind speed of 3.0 m/s at four different probe positions within the tank.

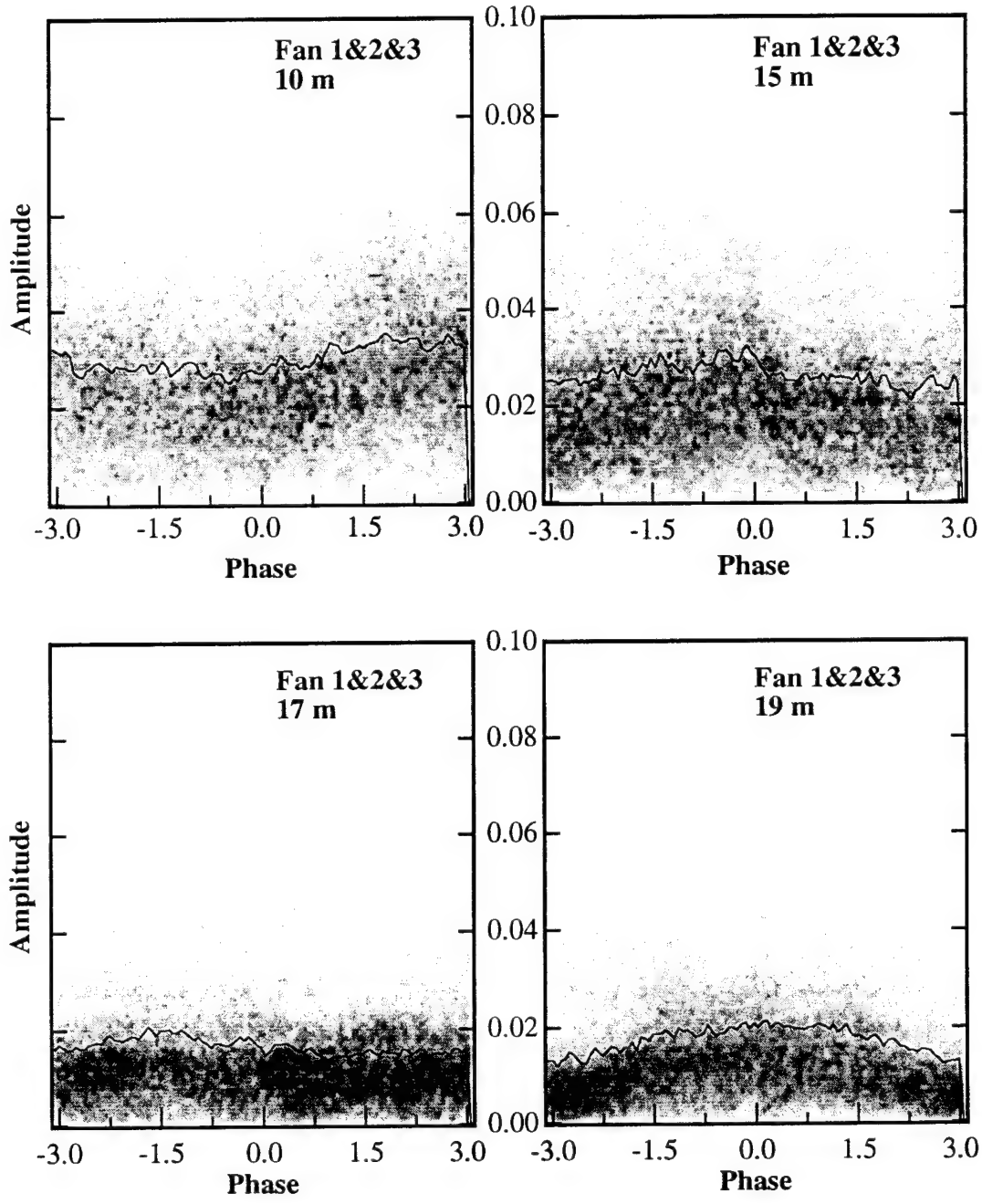

Figure 4-7. Distribution Plots of Amplitude of chop vs Phase of swell for a wind speed of 5.0 m/s at four different probe positions within the tank.

V. SURFACE TENSION

A. BACKGROUND

Surface tension of the tank has also been a concern during this experiment. Due to the large amount of redwood in the tank, accumulated grime on the walls, and brown color of the water, it was thought that the surface tension might vary substantially from that of pure water and should be measured. However, the ocean itself is obviously not pure water, so deviations from the pure water value may not be serious. Before attempting to measure the surface tension of the tank water, it was first necessary to understand how surface tension affects surface gravity waves. Gravity waves, which are driven by a balance between a fluid's inertia and its tendency under gravity to return to a state of stable equilibrium, are a principal example of dispersive waves. Disturbances to this state of equilibrium take the form of surface gravity waves that do not have much motion away from the surface - the motion in deep water decays exponentially with a characteristic length of wavelength/2π (Lighthill, 1978). Dispersion, a dependence of wave speed upon wavelength, is caused by the wavelength dependence of the effective fluid inertia associated with a depth of penetration.

The surface tension T serves as an additional restoring force measured as a force per length in units of Newtons per meter. By using the dispersion relation described earlier and adding the surface tension factor, the relationship can now be written as:

$$\omega^2 = \left(g + \rho^{-1} T k^2\right) k. \tag{5.1}$$

Surface tension measurements were made using the dispersion relationship shown in Equation 5.1 . By rearranging the terms, the equation can be rewritten as

$$T = \frac{4\pi^2 \rho}{k^3} f^2 - \frac{\rho g}{k^2} \tag{5.2}$$

B. MEASURING THE TANK SURFACE TENSION

Traveling wave techniques were attempted to establish a value for T in the tank. A Radio Shack 4″ Woofer with a small rod attached to the cone and a cork attached to the rod, as shown in Figure 5-1, was driven by a Stanford Research System Model DS335 Synthesized Function Generator. By varying the frequency, radial surface waves were produced on the water with various spacings between the rings. After the first few rings, the Hankel function $H_o^{(1)}(kr)$ describing cylindrical waves approaches e^{ikr} to high accuracy, where r is the radial distance, so k can be obtained from $2\pi / \lambda$, where λ is the ring separation at large r. Substituting k into Equation 5.2, along with other known quantities, gives the surface tension T.

For a first attempt to measure the rings, a bright LED light mount, strobscopically driven by a Hewlett Packard 33120A Function/Arbitrary Waveform Generator, was assembled. The angle and distance in which the LED's illuminated the rings proved to be crucial. Because of the optics involved, the ring patterns were very sporadic in behavior and trying to use calipers to measure separation distance was very inconsistent.

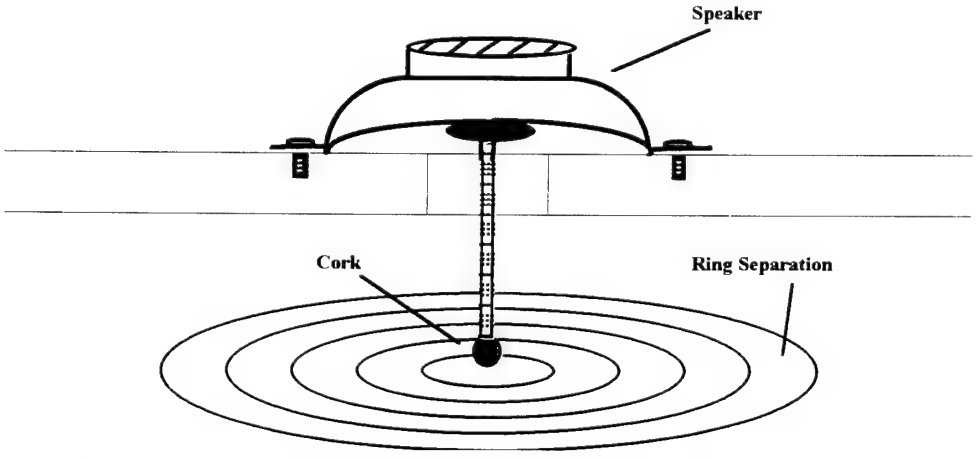

Figure 5-1. Speaker setup used to try and determine a value for k by measuring the ring separation of the waves produced by the cork which was driven by the speaker.

After other failed attempts, the method diagrammed in Figure 5-2 was used with success. The wave height probe used in the main experiments was mounted onto a railing system which controlled the position of the wave height probe. The speaker was vibration mounted with rubber bands onto the rail as well. A Lissajou pattern was produced on an oscilloscope between the probe output and the voltage driving the speaker. By sliding the probe along the railing radially with respect to the rings, the wavelength could be measured by noting the distance needed to have the Lissajou figure cycle through 360° of phase shift. Figure 5-2 is a block diagram of the system used to make this measurement. As shown in the diagram, the probe is powered and driven in the same manner described in Chapter II, Section E. To increase the sensitivity of the probe, a KROHN-HITE model 3322 filter was used and a 20 dB gain added. The low and high pass filters were adjusted according to the driving frequency of the speaker, which was driven by a Techron 5507 Power Supply Amplifier in series with a Function Generator.

From the wavelength, a value for k obtained, and the surface tension for the wave tank was calculated using Equation 5.2. Table 5-1 shows the results for surface tension measured for three different frequencies and then averaged. These values do not vary dramatically from the value of 0.074 N/m for pure water.

Frequency (Hz)	1	2	Average (N/m)
10	.102	.093	.098
15	.074	.078	.076
20	.085	.126	.105

Overall Tank Average (three frequencies):	.093
Overall Tank Average (two frequencies, 10 and 15 Hz:):	.087

Table 5-1. Surface Tension measurements made in the wind-wave tank.

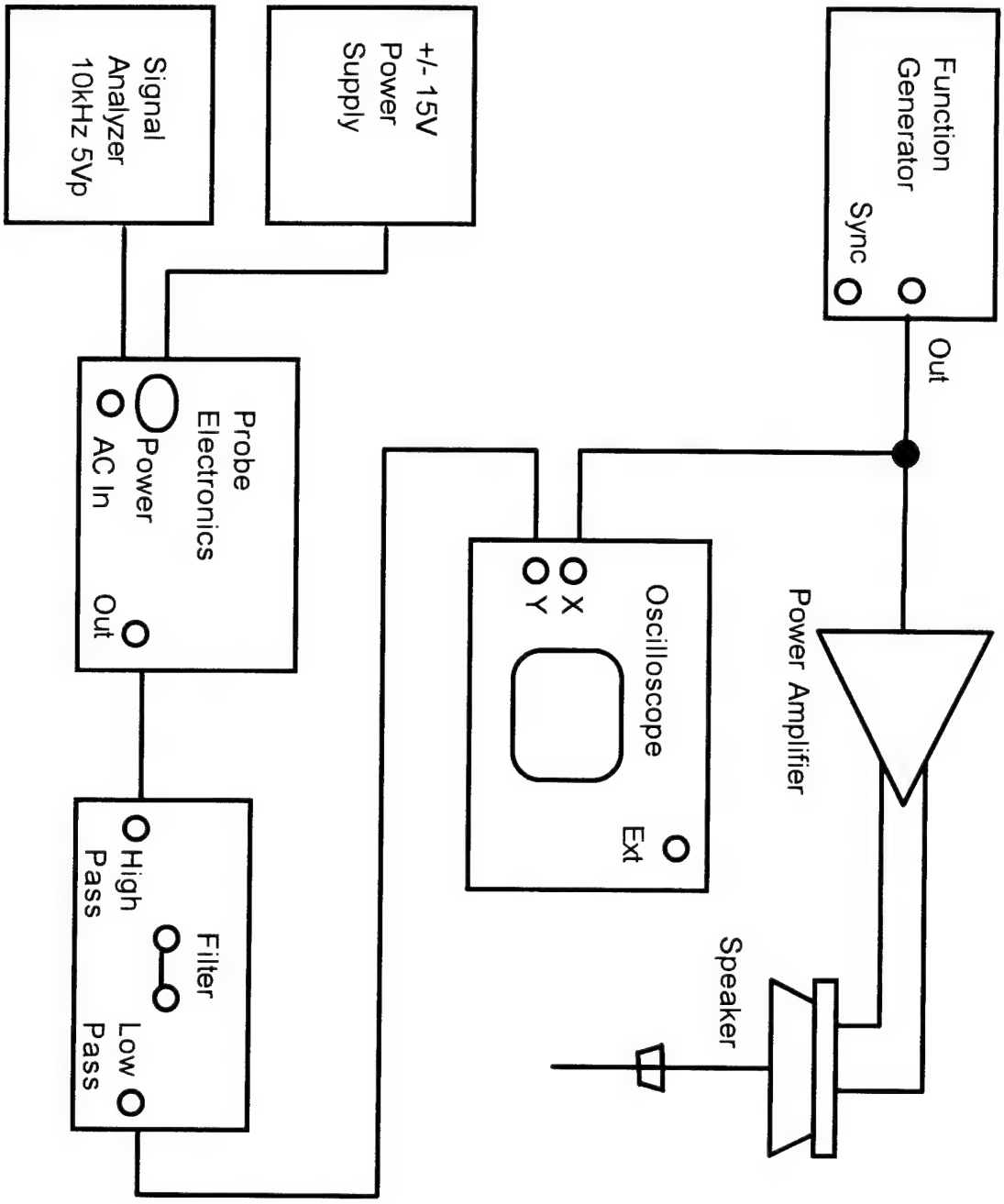

Figure 5-2. Block Diagram of the system used to measure the wavelength at various frequencies within the tank.

Figure 5-3 shows the relationship of the phase velocity in meters per second to the wave number in inverse meters for deep gravity - surface tension waves for pure water and the water in the wind-wave tank. Pure water is represented by the solid line while the tank water is represented as the dashed line which in this case is the average of two frequencies as shown in Table 5.1.

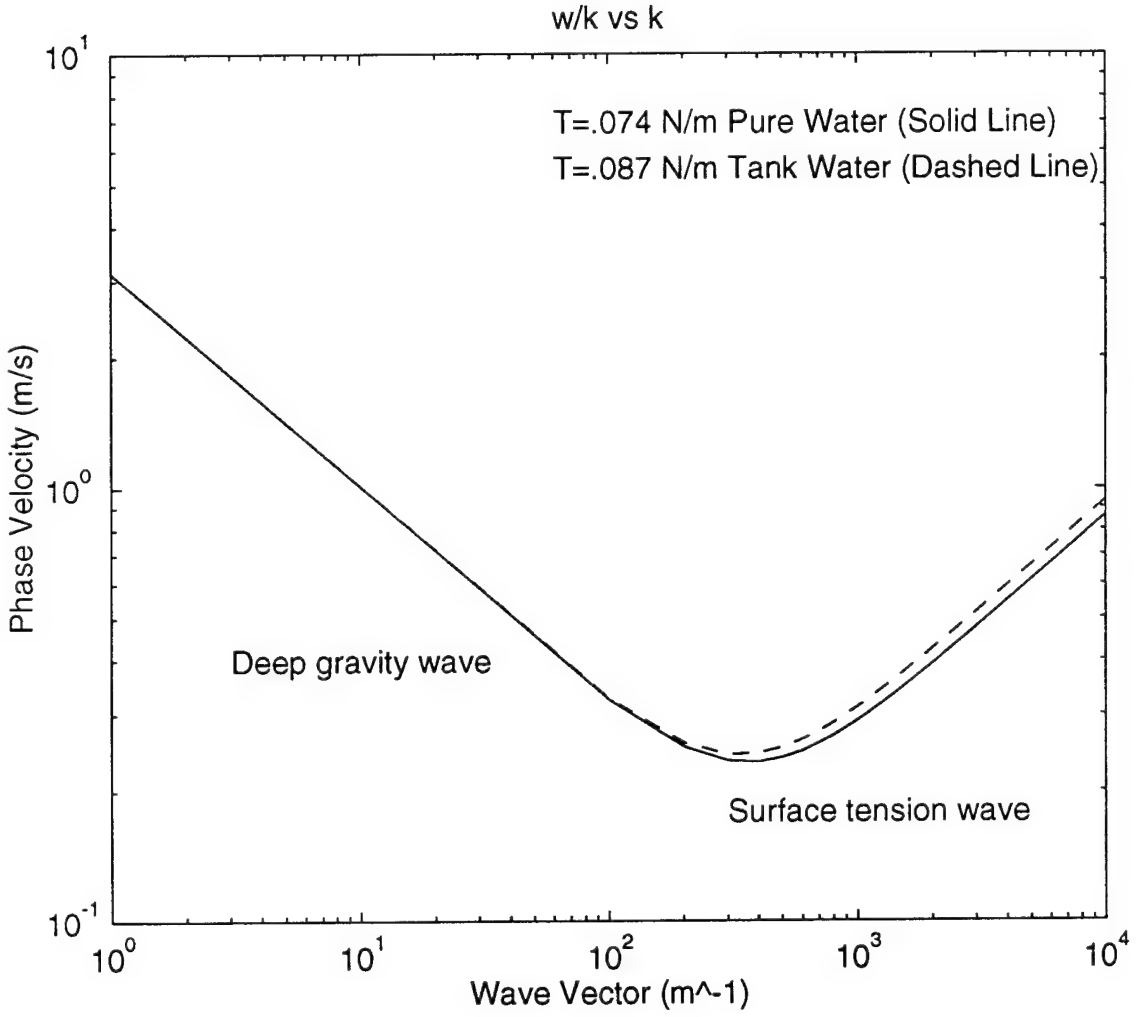

Figure 5-3. Relationship of the phase velocity in meters per second to the wave number in inverse meters for deep gravity - surface tension waves for pure water and water in the wind-wave tank.

VI. CONCLUSIONS AND FUTURE WORK

The burst propagation experiment produced valuable wind-wave tank data that, although not conclusive evidence of the collective mode itself, provided information on the affects wind speed and probe position may play on seeing the collective mode. These factors were even more evident during the mode coupling experiment in which results have yet to be explained. Specifically, determining why wind speed and probe position had such strange affects on the phase of the swell would possibly provide some answers in how to isolate the collective mode.

In future studies, it is hoped that new probes being made will allow data to be collected at several positions simultaneously. Since the probes will be distributed along the length of the tank, it would no longer be necessary to conduct single data runs which was very time consuming and tedious. The condition of the new probe will also be beneficial since the current probe is showing signs of corrosion and tension loss in the wires.

Two main areas were identified during this thesis study as limitations that could have influenced the results. The first is the actual frequencies input at the paddle. Although some narrowband frequencies were tried, this study dealt mainly with broadband frequencies which may not be ideal in identifying the collective mode. A second factor was restrictions introduced by the depth of the wind-wave tank. A larger, deeper tank may allow the mode coupling experiment to be performed with different ratios of gravity wave to collective mode frequencies.

APPENDIX. WAVE TANK SIGN TEST

An experiment was conducted to ensure that the circuitry of the wave height probe and Davies' (1994) software had not somehow introduced an inversion error which would give a phase error of π. The experiment was conducted using the modified Waveturb 1.4 Panel LabVIEW program at 2048 counts per channel. Repeatedly, the crest of the swell was simulated by manually pushing the wave height probe down into the tank of still water for about one second while jiggling the probe up and down to simulate the chop. The probe was pulled up and held as still as possible for a five second period to simulate little or no chop in the trough of the swell. Using Davies' processing programs, Figure A-1 shows the time domain plot. The upper plot shows the one-to-five second ratio of the crest to trough. As discussed by Davies, by comparing the two lower plots one can see that the largest amplitude modulations of the simulated chop are occurring at the crests of the simulated swell. Then by processing this data with the Spyglass Transform and Format tools, the distribution plot of the amplitude of the chop and the phase of the swell along with the rms average of the chop amplitude clearly shows the largest chop amplitude occurring at the crests of the swell, Figure A-2. Therefore, the measurements taken in the wave tank do not contain an inversion error. The cutoff frequencies used were 0.5 Hz for the low pass filter and 1.5 Hz for the high pass filter.

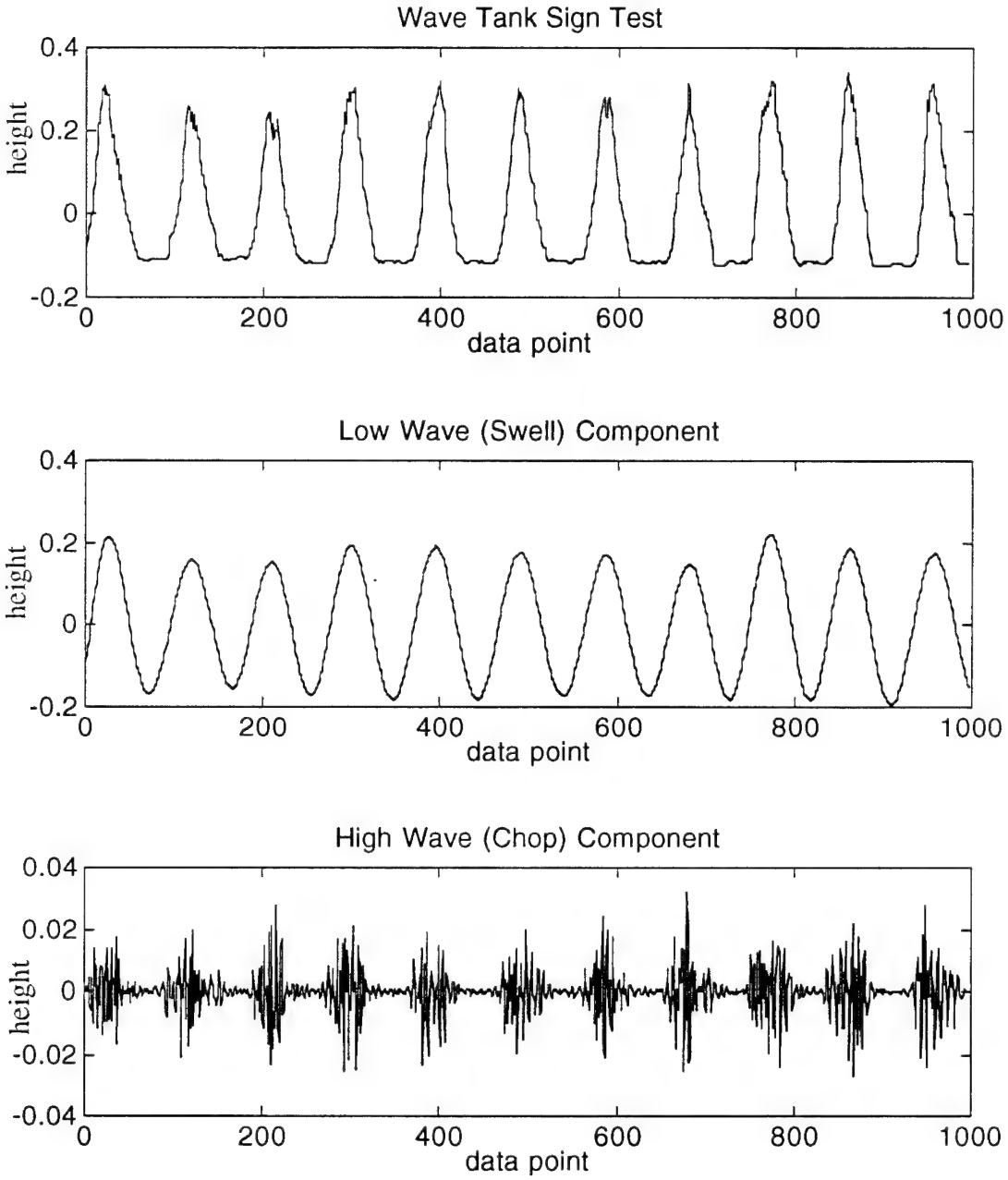

Figure A-1. Wave Tank Data Sign Test.
Sign test as conducted for Davies (1994) repeated with most current data to verify that no inversion error has been introduced. Swell cutoff frequency is 0.5 Hz. Chop cutoff frequency is 1.5 Hz.

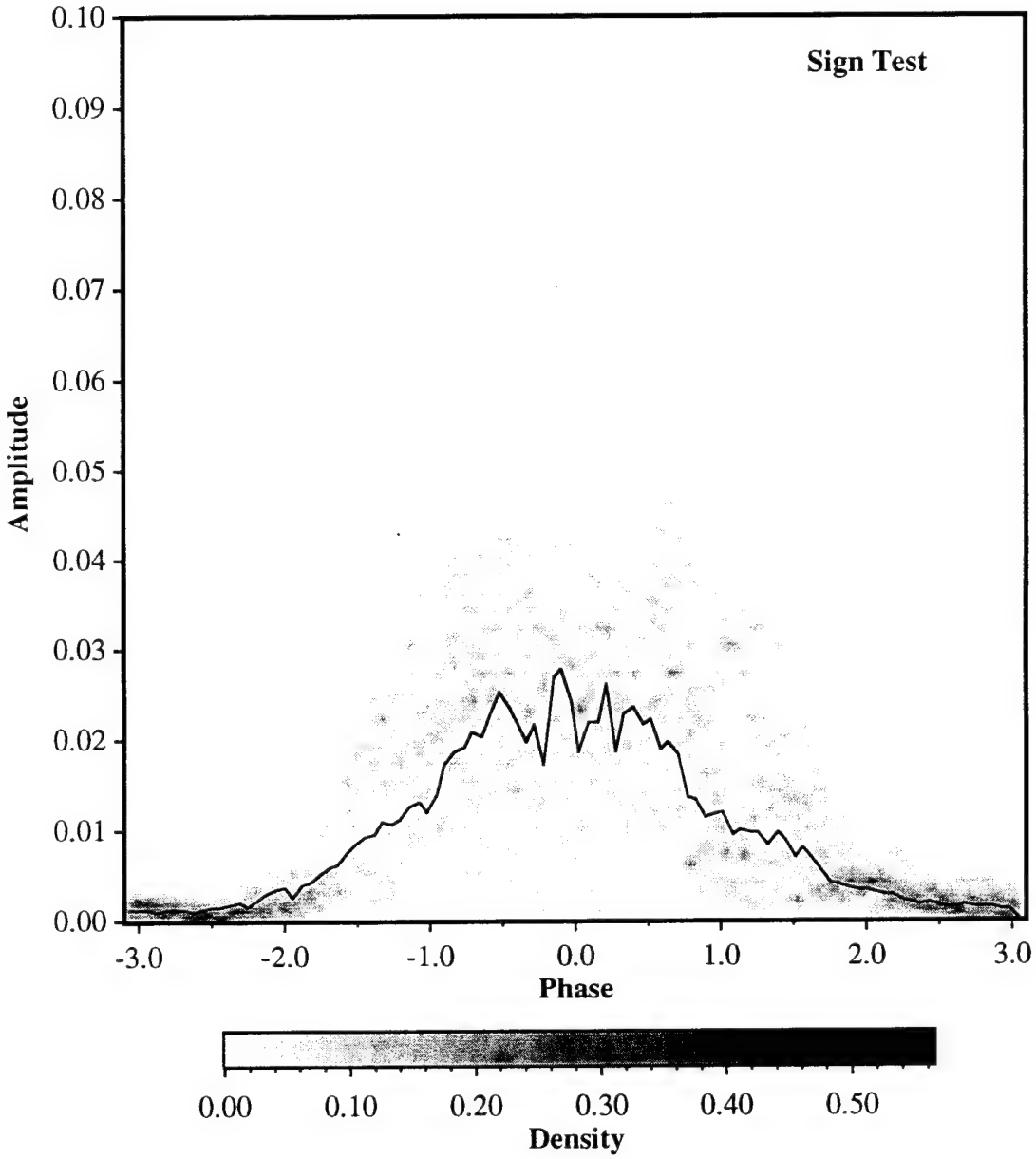

Figure A-2. Distribution Plot of Amplitude of chop vs Phase of swell for Wave Tank Sign Test. The solid line is the RMS amplitude of the chop. The largest chop amplitude is again at the crests of the swell as was shown by Davies (1994) thus verifying that the measurements do not contain an inversion error.

LIST OF REFERENCES

Davies, J., "Techniques for the Investigation of Wave Turbulence in Water Wave Data," Masters Thesis, Naval Postgraduate School, Monterey, CA, September 1994.

LabVIEW for Macintosh User and Reference Manual, Version 3.0, August 1993 Edition, National Instruments Corporation, Austin, TX, 1993.

Larraza, A., "Physical Applications of Wave Turbulence: Wind Waves and Classical Collective Modes," Chapter 5, pp. 84-94, Burkhauser Boston, 1993.

Larraza, A. and Falkovich, G., "Collective Modes in Open Systems of Nonlinear Random Waves," *Phys. Rev B* Vol48, No. 13, pp. 9855-9857, 1993.

Larraza, A., Garrett, S.L. and Putterman, S., "Dispersion Relations for Gravity Waves in a Deep Fluid: Second Sound in a Stormy Sea," *Phys. Rev A* Vol41, pp. 3144-3155, 1990.

Lawrence, R., "Experimental Inquires Into Collective Sea State Modes in Deep Water Gravity Waves," Masters Thesis, Naval Postgraduate School, Monterey, CA, December 1992.

Lighthill, J., "Waves in Fluids," Chapter 3, Cambridge University Press, pp. 205-206, 1978.

Spyglass Format Quick Tour and Reference, Version 1.1, Second Edition, Spyglass, Inc., Champaign, IL, 1991.

Spyglass Transform Quick Tour and Reference, Version 3.01, Fourth Edition, Spyglass, Inc., Champaign, IL, 1993.

Yarber, K., "Development and Calibration of Two and Four Wire Water Surface Wave Height Measurement Systems," Masters Thesis, Naval Postgraduate School, Monterey, CA, December 1992.

Zakharov, V., Lvov, V. and Falkovich, G., "Kolmogorov Spectra of Turbulence," V.1 Wave Turbulence, Springer-Verlag, 1992.

INITIAL DISTRIBUTION LIST

1. Defense Technical Information Center.....2
   Cameron Station
   Alexandria, VA 22304-6145

2. Library, Code 52.....2
   Naval Postgraduate School
   Monterey, CA 93943-5101

3. Professor Robert M. Keolian.....2
   Physics Department, Code PH/Kn
   Naval Postgraduate School
   Monterey, CA 93943

4. Professor Andres Larraza.....1
   Physics Department, Code PH/La
   Naval Postgraduate School
   Monterey, CA 93943

5. Dr. Michael F. Shlesinger.....1
   Office of Naval Research, Code 331
   800 N. Quincy Street
   Arlington, VA 22217-5660

6. LT Patricia A. Gill, USN.....1
   HSL-45
   NAS North Island
   San Diego, CA 92132

7. Dr. Mark A. Donelan.....1
   National Water Research Institute,
   Canada Centre for Inland Waters,
   Burlington, Ontario, Canada L74 4A6

8. Professor Gregory Falkovich.....1
   Department of Physics
   Weizmann Institute of Science
   Rehovot 76100, Israel

9. Professor Seth Putterman 1
Department of Physics
University of California, Los Angeles
405 Hilgard Avenue
Los Angeles, CA 90024-1547